



Aalto University



Micro and Quantum Systems

ELEC-C9440 Quantum Information

# Quantum memory and applications of quantum optics

Vladimir V. Kornienko

[vladimir.kornienko@aalto.fi](mailto:vladimir.kornienko@aalto.fi)

31.05.2023

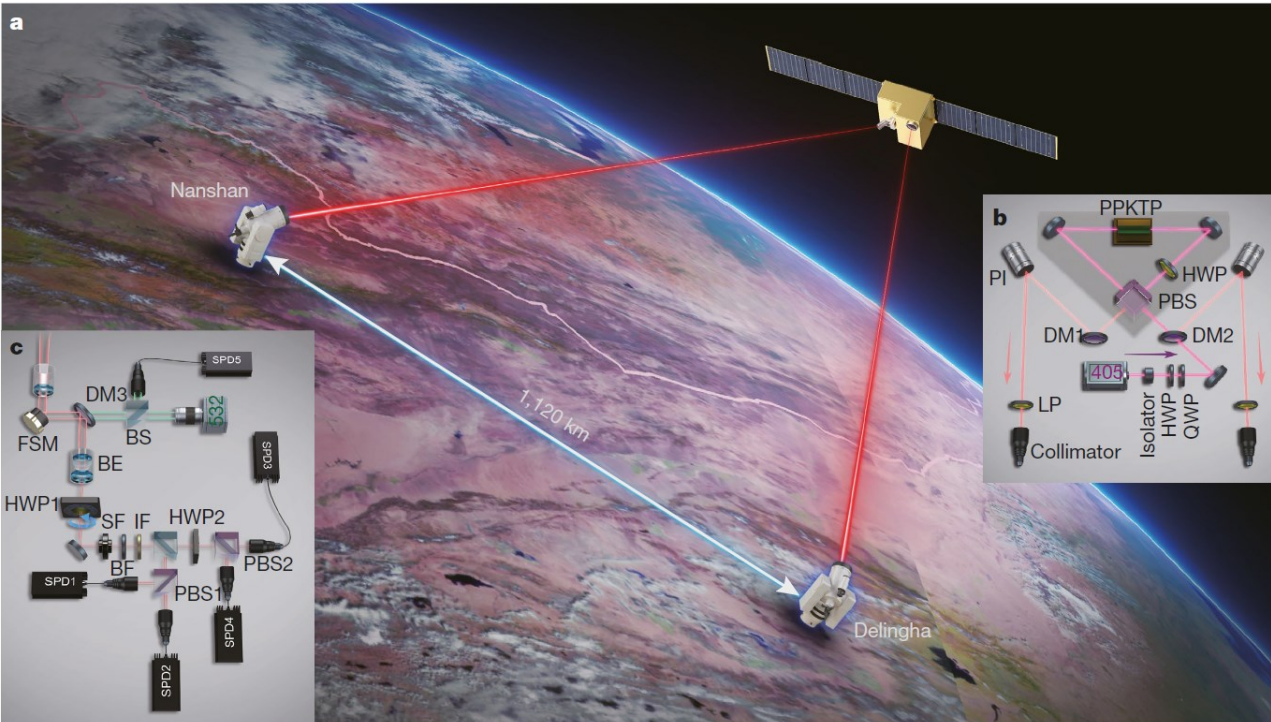


**Fig. 1 | Overview of the experimental set-up of entanglement based quantum key distribution.** **a**, An illustration of the Micius satellite and the two ground stations. Image credit: Fengyun-3C/Visible and Infrared Radiometer, with permission (2020). The satellite flies in a Sun-synchronous orbit at an altitude of 500 km. The physical distance between Nanshan and Delingha ground station is 1,120 km. **b**, The spaceborne entangled-photon source. A free space isolator is used to minimize back reflection to the 405-nm pump laser. A pair of off-axis concave mirrors is used to focus the pump laser and collimate the down-converted photon pairs. PBS, polarization beam splitter; DM,

dichroic mirror; LP, long-pass edge filter; PI, piezo steering mirror; HWP, half-wave plate; QWP, quarter-wave plate; PPKTP, periodically poled KTiOPO<sub>4</sub>. **c**, The follow-up optic at the optical ground station. The tracking and synchronization laser is separated from the signal photon by DM3 and detected by the single photon detector (SPD5). The spatial filter (SF), broad-bandwidth filter (BF) and interference filter (IF) are used to filter out the input light in frequency and spatial domains. BS, beam splitter; BE, beam expander; FSM, fast steering mirror.

[ J. Yin et al., “Entanglement-based secure quantum cryptography over 1,120 kilometres” // *Nature* **582**, 501-505 (2020). <https://doi.org/10.1038/s41586-020-2401-y> ]

# 'Quantum Internet' Inches Closer With Advance in Data Teleportation

Scientists have improved their ability to send quantum information across distant computers — and have taken another step toward the network of the future.

[ <https://www.nytimes.com/2022/05/25/technology/quantum-internet-teleportation.html> ]

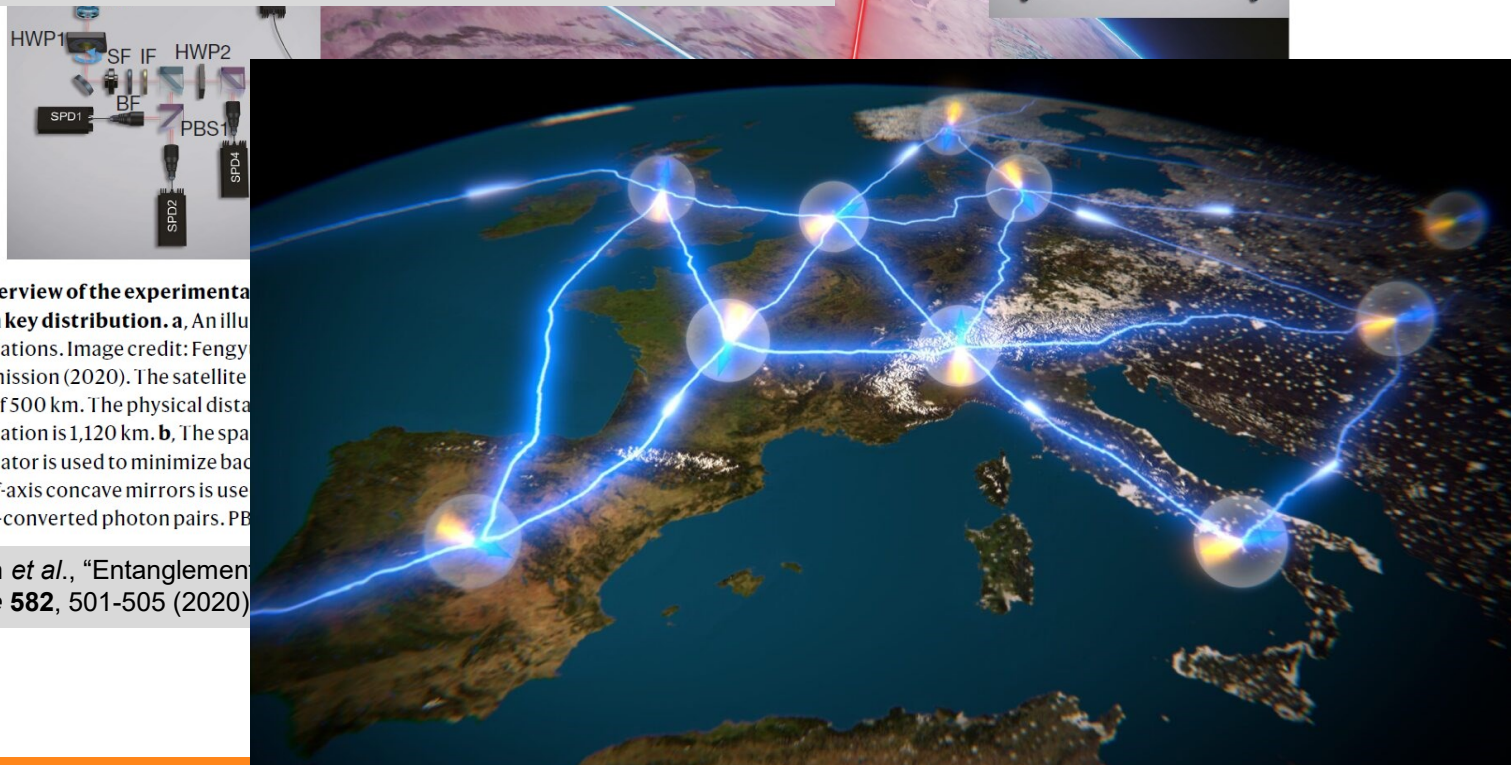


**Fig. 1 | Overview of the experimental quantum key distribution.** **a**, An illustration of the ground stations. Image credit: Fengyuan et al. (2020) with permission (2020). The satellite is at an altitude of 500 km. The physical distance between the ground station and the satellite is 1,120 km. **b**, The space isolator is used to minimize background noise. A pair of off-axis concave mirrors is used to collect the down-converted photon pairs. PBS, polarizing beam splitter; HWP, half-wave plate; SF, spatial filter; IF, interference filter; BF, beam splitter; SPD, single-photon detector.

[ J. Yin et al., "Entanglement Distribution via Satellite for Global Quantum Key Distribution," *Nature* **582**, 501-505 (2020) ]

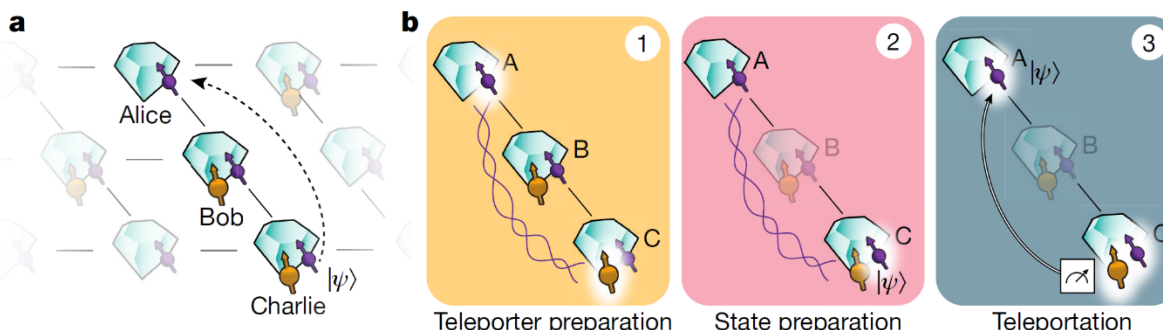


**Fig. 1 | Teleporting a qubit between non-neighbouring nodes of a quantum network.** **a**, Three network nodes, Alice (A), Bob (B) and Charlie (C), are connected by means of optical fibre links (lines) in a line configuration. Each setup has a communication qubit (purple) that enables entanglement generation with its neighbouring node. Furthermore, Bob and Charlie contain a memory qubit (yellow). **b**, The steps of the teleportation protocol. (1) We prepare the teleporter by establishing entanglement between Alice and Charlie

using an entanglement swapping protocol on Bob, followed by swapping the state at Charlie to the memory qubit. (2) The qubit state to be teleported is prepared on the communication qubit on Charlie. (3) A BSM is performed on Charlie's qubits and the outcome is communicated to Alice over a classical channel. Dependent on this outcome, Alice applies a quantum gate to obtain the teleported qubit state.

[S.L.N. Hermans *et al.*, “Qubit teleportation between non-neighbouring nodes in a quantum network” // *Nature* **605**, 663-668 (2022).  
<https://doi.org/10.1038/s41586-022-04697-y>]

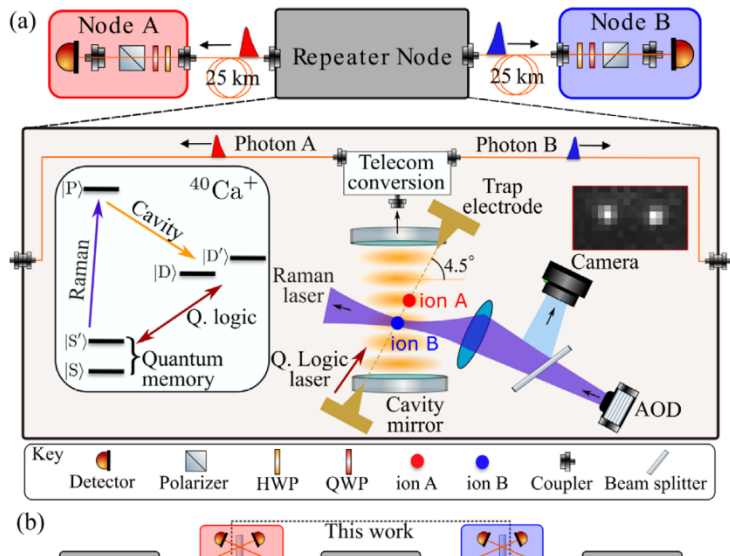


**FIG. 2. Trapped-ion quantum repeater node.** **(a)** Experimental schematic of an elementary network segment containing one repeater node. Photonic nodes A and B are each sent a telecom-converted [50,51] 1550 nm photon, entangled with a different ion, via 25-km-long fiber spools. Ion-qubit readout is done via imaging ion fluorescence at 397 nm on a camera. Ion-qubit quantum logic (Q. logic) gates are done via a 729 nm laser that couples equally to the ions. AOD, acousto-optic deflector; HWP, half-wave plate; QWP, quarter-wave plate. Level scheme:  $|S\rangle = |4^2S_{1/2,m_j=-1/2}\rangle$ ,  $|S'\rangle = |4^2S_{1/2,m_j=+1/2}\rangle$ ,  $|P\rangle = |4^2P_{3/2,m_j=-3/2}\rangle$ ,  $|D\rangle = |3^2D_{5/2,m_j=-5/2}\rangle$ ,  $|D'\rangle = |3^2D_{5/2,m_j=-3/2}\rangle$ . **(b)** Envisioned concatenation of the network segment in (a) into a repeater chain. Photon detection heralds remote ion entanglement [52].

[ V. Krutyanskiy *et al.*, “Telecom-Wavelength Quantum Repeater Node Based on a Trapped-Ion Processor” // *Phys. Rev. Lett.* **130**, 213601 (2023).  
<https://doi.org/10.1103/PhysRevLett.130.213601> ]

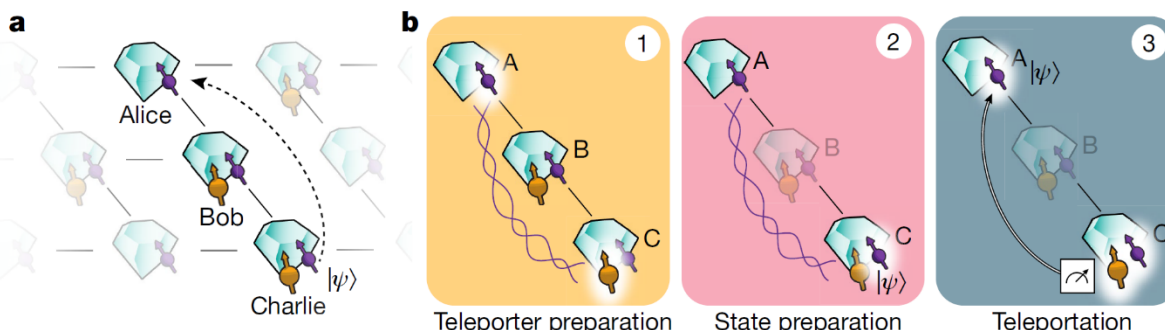


**Fig. 1| Teleporting a qubit between non-neighbouring nodes of a quantum network.** **a**, Three network nodes, Alice (A), Bob (B) and Charlie (C), are connected by means of optical fibre links (lines) in a line configuration. Each setup has a communication qubit (purple) that enables entanglement generation with its neighbouring node. Furthermore, Bob and Charlie contain a memory qubit (yellow). **b**, The steps of the teleportation protocol. (1) We prepare the teleporter by establishing entanglement between Alice and Charlie

using an entanglement swapping protocol on Bob, followed by swapping the state at Charlie to the memory qubit. (2) The qubit state to be teleported is prepared on the communication qubit on Charlie. (3) A BSM is performed on Charlie's qubits and the outcome is communicated to Alice over a classical channel. Dependent on this outcome, Alice applies a quantum gate to obtain the teleported qubit state.

[S.L.N. Hermans *et al.*, “Qubit teleportation between non-neighbouring nodes in a quantum network” // *Nature* **605**, 663-668 (2022).  
<https://doi.org/10.1038/s41586-022-04697-y>]

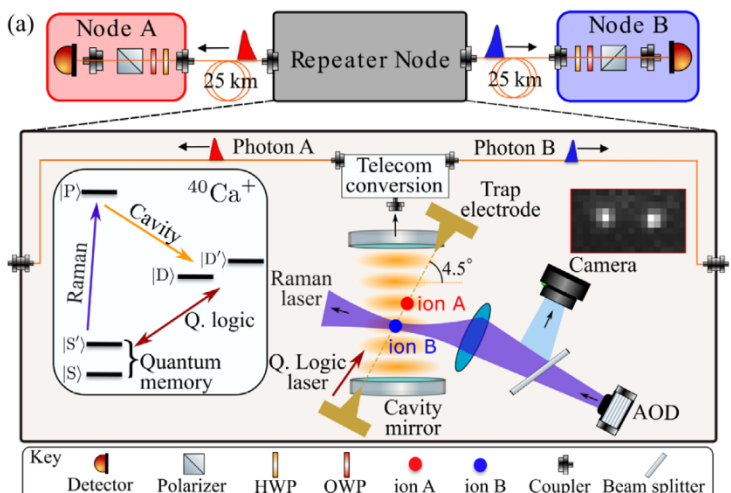
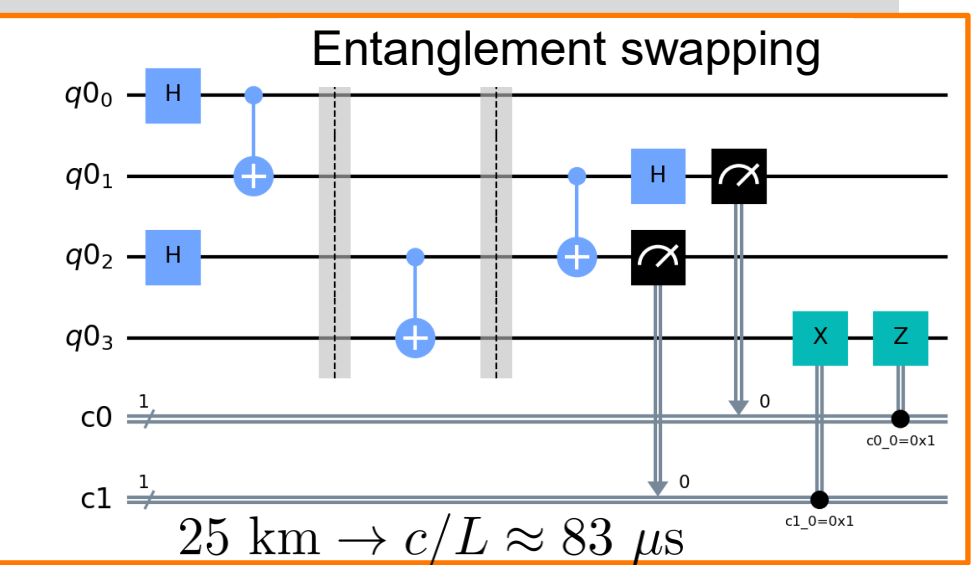


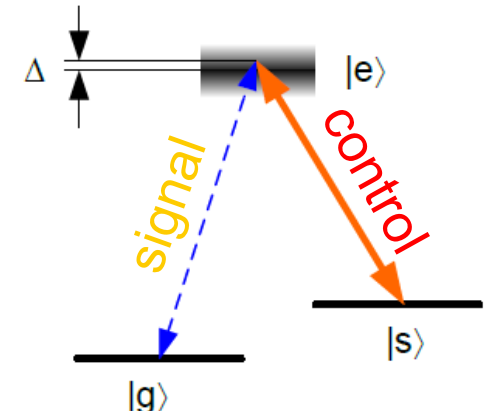
FIG. 2. schematic repeater converted via 25-km ion fluo (Q. logi the ions QWP, c |S'⟩ = |3<sup>2</sup>D<sub>5/2</sub>. enation detectio



[ V. Krutyanskiy *et al.*, “Telecom-Wavelength Quantum Repeater Node Based on a Trapped-Ion Processor” // *Phys. Rev. Lett.* **130**, 213601 (2023).  
<https://doi.org/10.1103/PhysRevLett.130.213601> ]

# Outline

- ❑ Quantum Memory (QM):  
Introduction and Types
- ❑ Cavity-based QM
- ❑ Applications of Quantum Optics
  - ❑ Beam-splitter transfer matrix
  - ❑ Field operator transformation for a beam-splitter
  - ❑ Calculating the output field state
  - ❑ Hong-Ou-Mandel interference
  - ❑ Mach-Zehnder Interferometer
- ❑ Media-based QM



[ G. Gilbert, A. Aspect, C. Fabre. (2010). *Introduction to Quantum Optics*. New York: Cambridge University Press. ]

[ A.M. Kelley. (2012). *Condensed-Phase Molecular Spectroscopy and Photophysics*. New Jersey: John Wiley & Sons, Inc. ] (Sec. 8.8, “Solvent Effects on Electronic Spectra”)

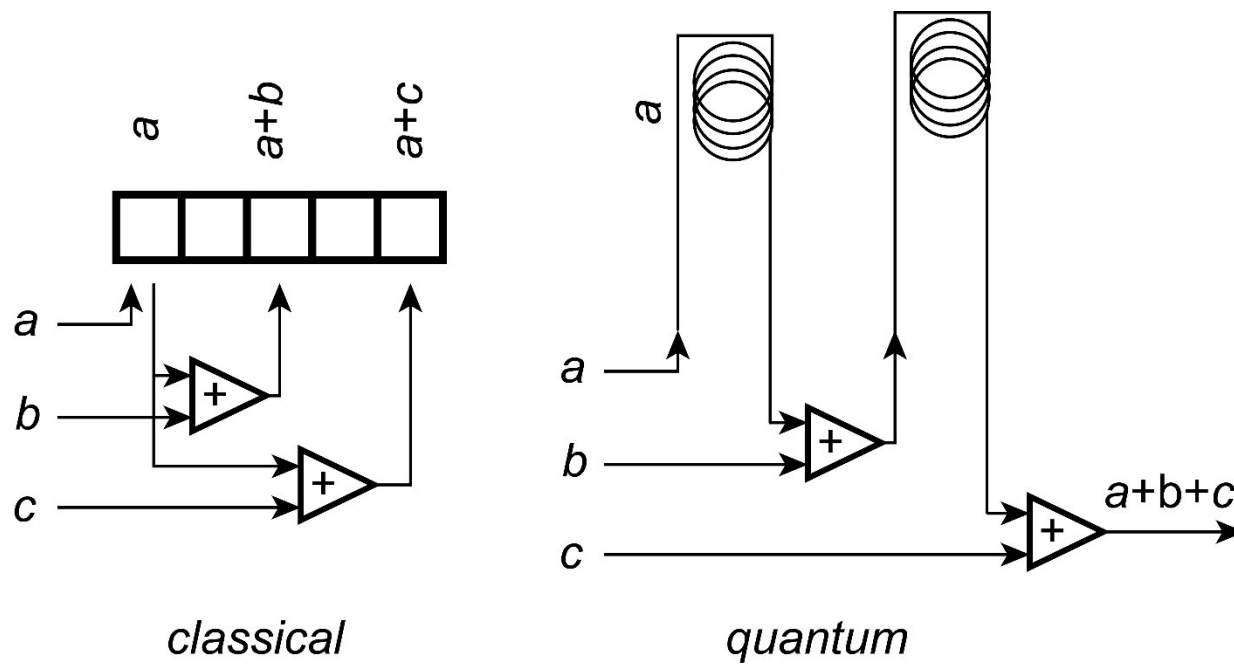
[ D. Klyshko. (2011). Physical Foundations of Quantum Electronics. (Eds. M. Chekhova, S. Kulik). <https://doi.org/10.1142/7930> ]

[A. Yariv. (1975). *Quantum Electronics* (2nd ed.). New York: John Wiley & Sons. ]

# Quantum memory (QM)

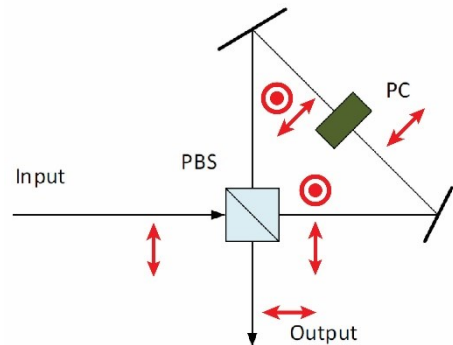
- A mean of storing the information in quantum computing.
- A device for storing quantum information.
- Can enhance the performance of probabilistic quantum sources / gates and assist in preparing complex non-classical states.

QM can temporarily store a quantum state, and then retrieve it on demand later.

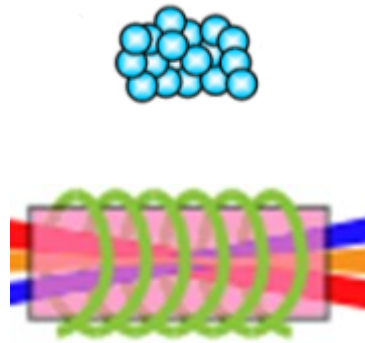


# Quantum memory (types):

## □ Cavity-based



## □ Media-based



Physical platforms for QM:

- cold ions in a trap
- rare-earth ion-doped solids
- diamond color centers
- crystalline solids (?)
- molecules
- alkali metal vapours

## Other applications:

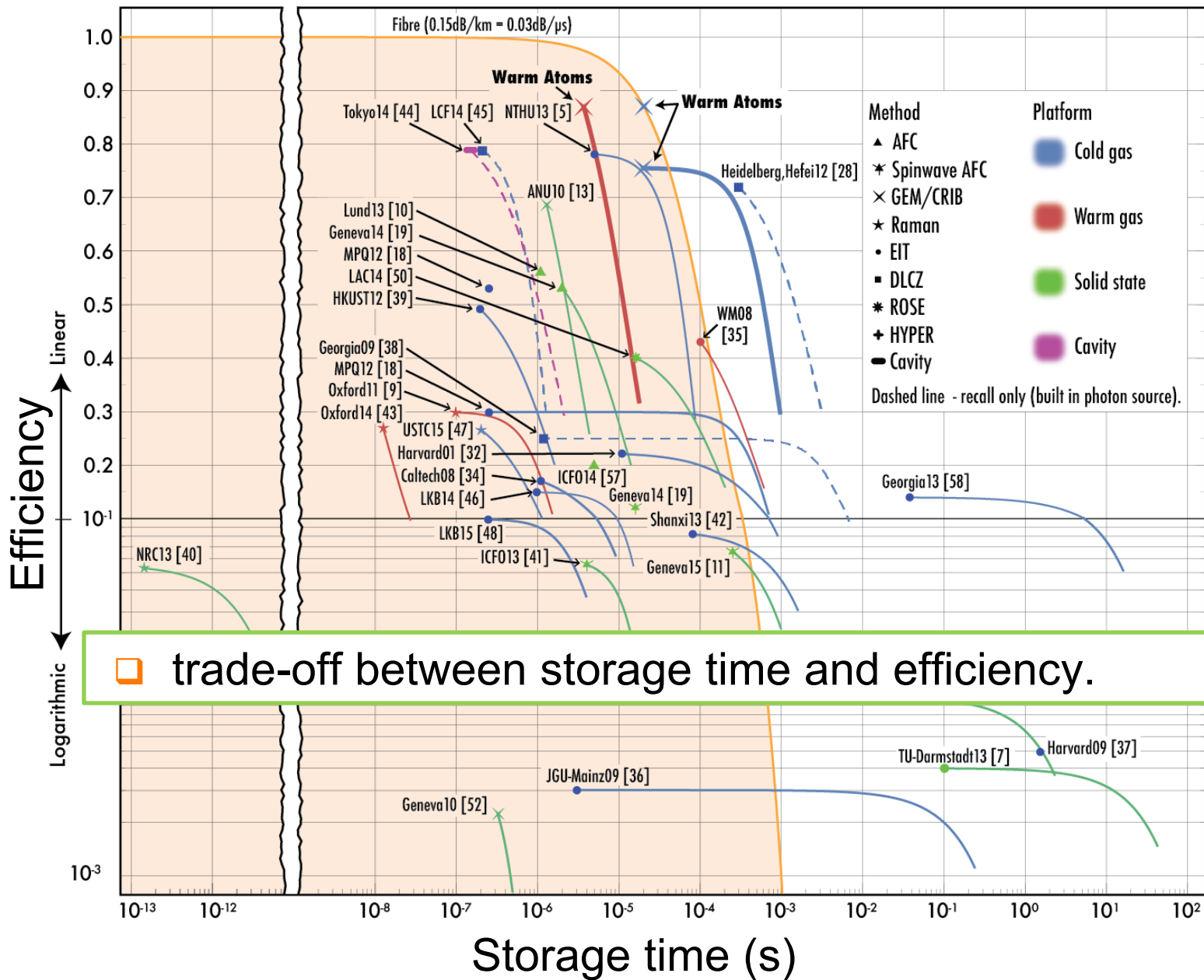
- ❖ Quantum-memory-assisted photon interference
- ❖ Measurement-device-independent quantum key distribution
- ❖ Quantum teleportation
- ❖ Quantum repeaters
- ❖ Fundamental tests in quantum mechanics (Bell's inequality)
- ❖ Quantum metrology, precise measurements
- ❖ Nonlinear interactions between systems

# Criteria for assessing QM performance

1. Efficiency
2. Fidelity, purity, trace distance
3. Storage time
4. Bandwidth
5. Wavelength, capacity, dimensionality

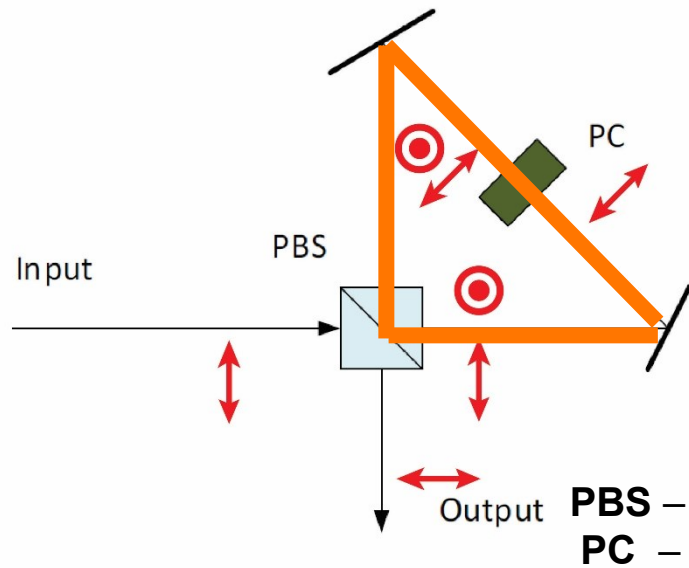
[ C. Simon *et al.*, "Quantum memories" // *Eur. Phys. J. D* **58**, 1–22 (2010); DOI: 10.1140/epjd/e2010-00103-y . ]

Approach	Potential Applications	Efficiency	Measurement	Fidelity	Entanglement with light	Band width	Storage Time	MM capacity	Dim.
RE AFC	SPS, QRep LOC4	0.34 ~1	retrieval	0.97 cond.	not yet Yes with PDC	100 MHz 1 GHz	15 µs 30 s	64 high	high
NV	QRep, SPS	not yet ~1 with cavity	direct	0.85	done	not yet 10 MHz	>100 µs >10 ms	moderate	moderate
QD	SPS, QRep	~0.04 ~1	retrieval	0.94	done	>GHz	2 ns 100 µs	high	low
Single atoms Free space	LHF, QRep	low ~1 with cavity	direct	0.94 cond.	done	6 MHz	150 µs >ms	moderate	moderate
Room-temp. gas	LOC4, Prec.msmt.	1	direct	0.7 uncond.	done	kHz 100 kHz	4 ms 200 ms	low	high
Cold gas	Prec.msmt., LOC4, QRep	1	direct	0.75 uncond.	not yet yes	1 MHz 0.5 GHz	not yet 100 ms	moderate (spatial)	high
Raman gas	SPS, QRep	0.15 ~1	retrieval	0.85 cond.	not yet yes	1 GHz GHz	2 µs >100 µs	moderate	high



[ Y.-W. Cho et al., "Highly efficient optical quantum memory with long coherence time in cold atoms" // 3 (1), 100-107 (2016). <https://doi.org/10.1364/OPTICA.3.000100> . ]

# Simplest quantum memory: a cavity



Light pulses are stored in a cavity, consisting of highly-reflecting mirrors and a control element for extracting the pulses out.

Vertically-polarized light is trapped in the cavity, and the horizontally polarized light can enter it and/or escape it. Light polarization can be changed with a Pockels cell – a nonlinear crystal to which the voltage pulse can be supplied.

Spacing  $\Delta t$  between adjacent pulses stored in the memory cannot be smaller than  $\min\{\tau_0, \tau_{PC}\}$ .

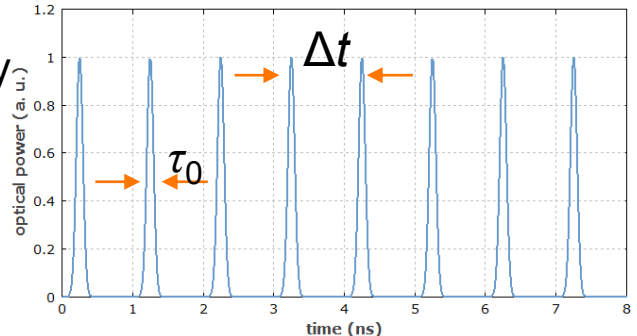
Cavity length  $L$  defines the cavity round-trip time and the maximum time interval available to a QM:

$$t_{MAX} = L_{tot} / c .$$

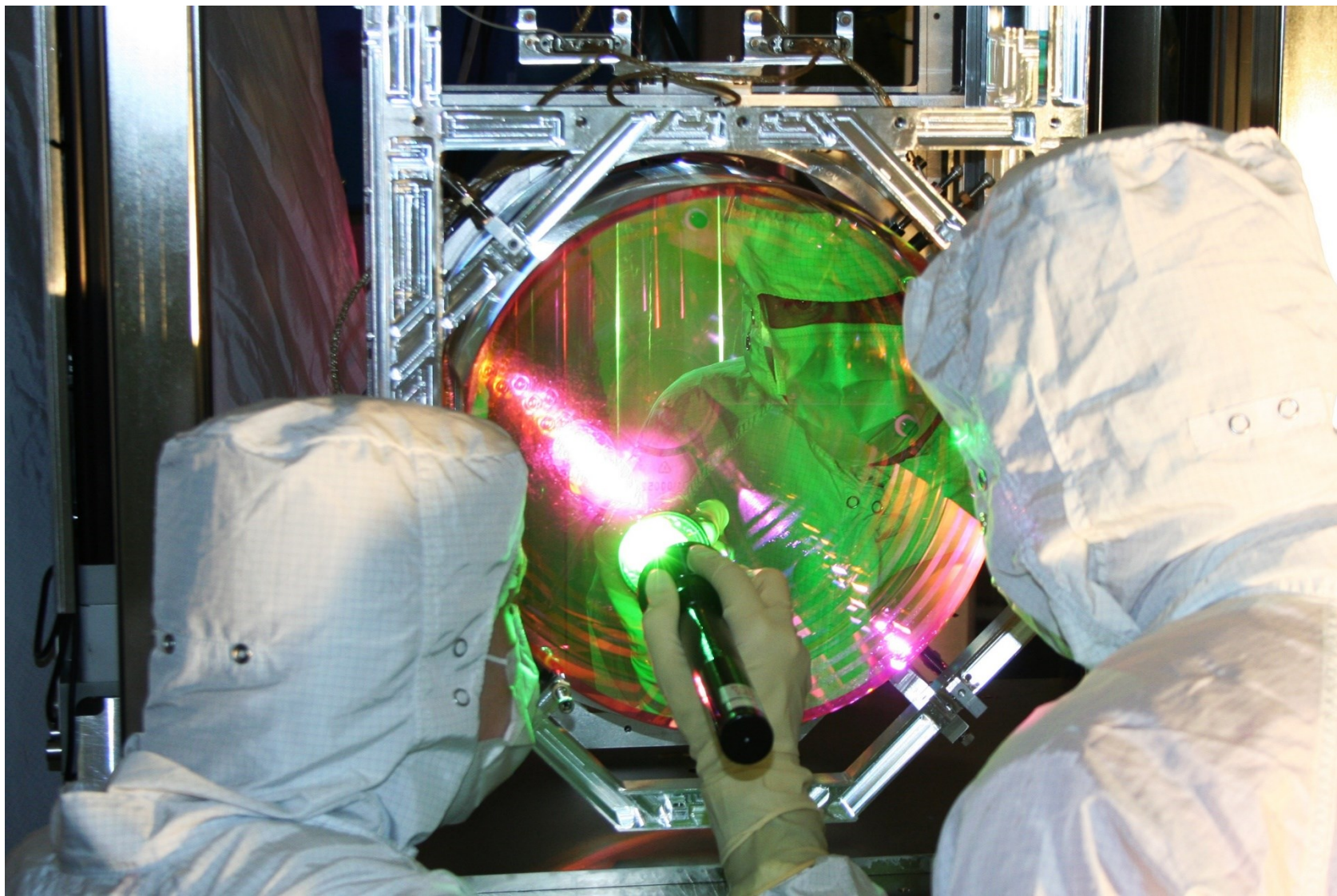
Capacity:  $N_{pulses} = t_{MAX} / \Delta t .$

Cavity overall transmittance  $T_{cav} = N_1 / N_0 :$   
how much pulses are lost per 1 round trip.

$\tau_0$  – pulse duration  
 $\tau_{PC}$  – Pockels cell switching time (on / off)



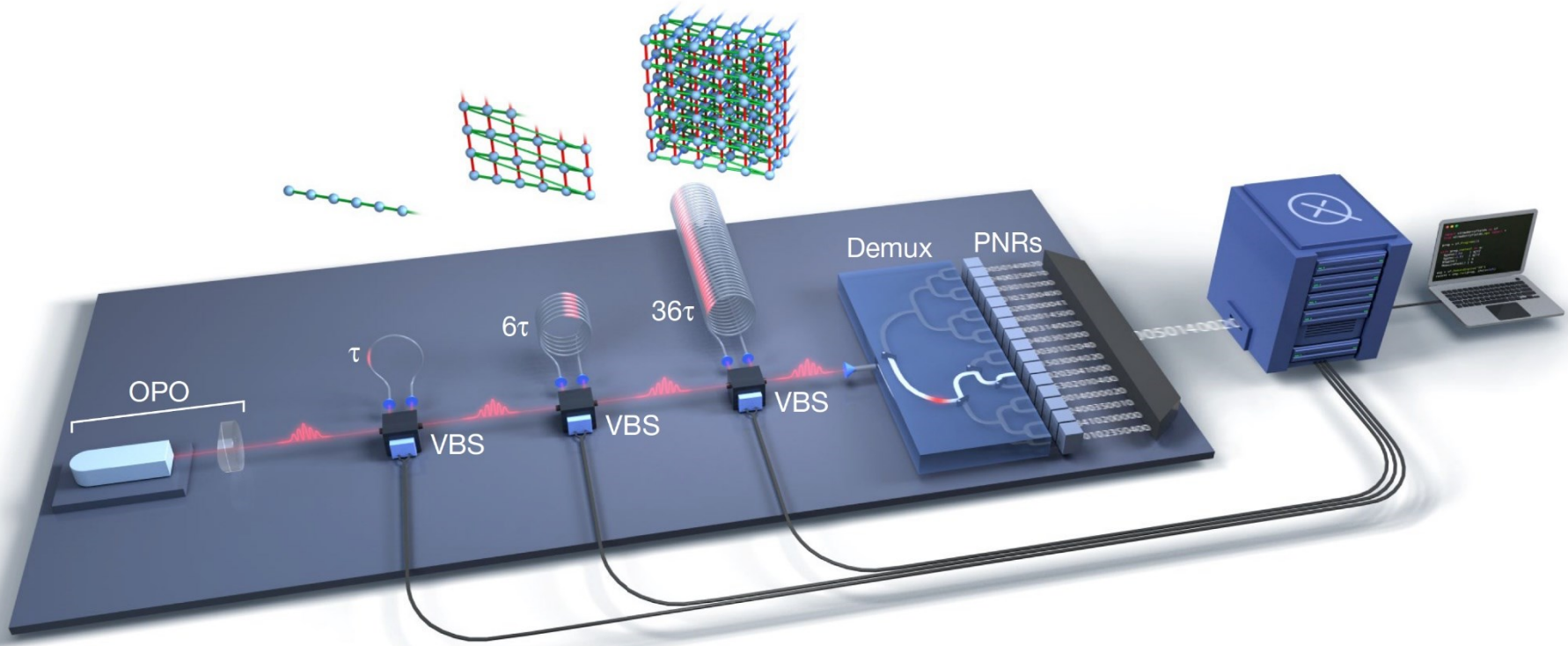
- + simple
- + broadband
- losses (storage time)
- cavity length (timing accuracy vs available pulse duration)



What's the expected quality of the optical elements in such a memory?

Example: main mirror in LIGO gravitational wave interferometer,  $T = 1 - 3e-7$ .

# A step further: linear optics for quantum computing

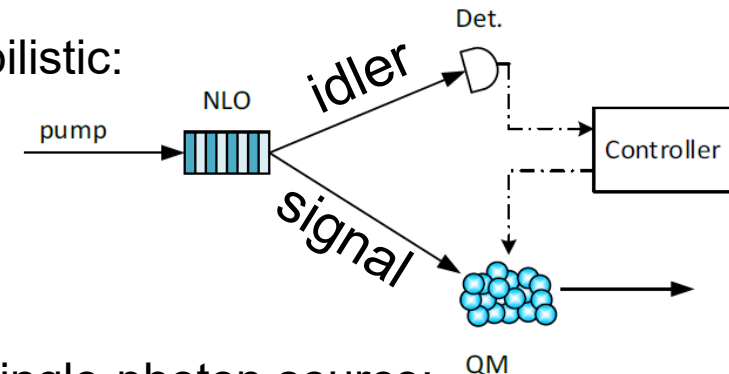


Programmable photonic processor by Xanadu (Toronto, Canada)

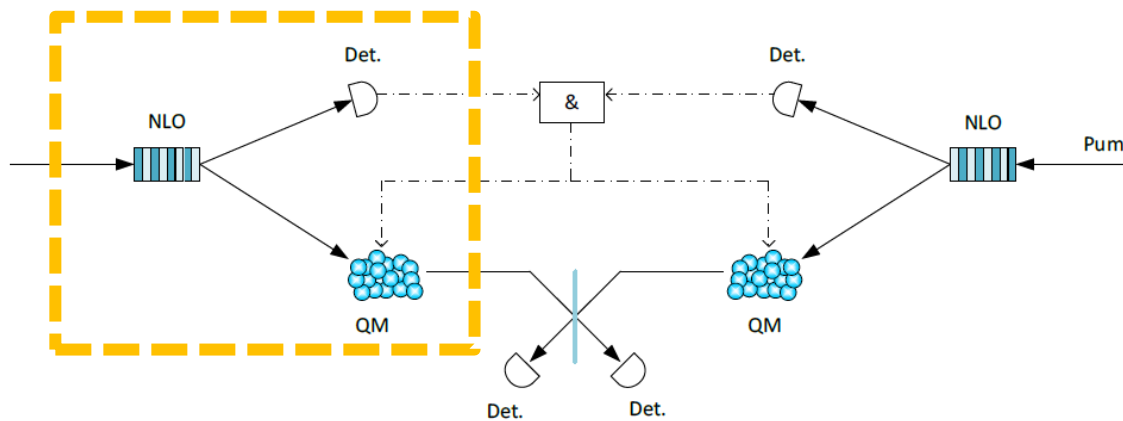
Gaussian boson sampling on 216 squeezed modes entangled with three-dimensional connectivity, using a time-multiplexed and photon-number-resolving architecture. Registering events with up to 219 photons and a mean photon number of 125.

# Applications – 1: QM-assisted multi-qubit states

- In the example, the creation of photons is probabilistic:  
spontaneous parametric down-conversion (SPDC);  
four-wave mixing (FWM);



- One photon of the pair is detected, heralding the arriving of the other one;
- Use quantum memory to create a deterministic single-photon source;
- Improves the performance of multi-channel experiments:

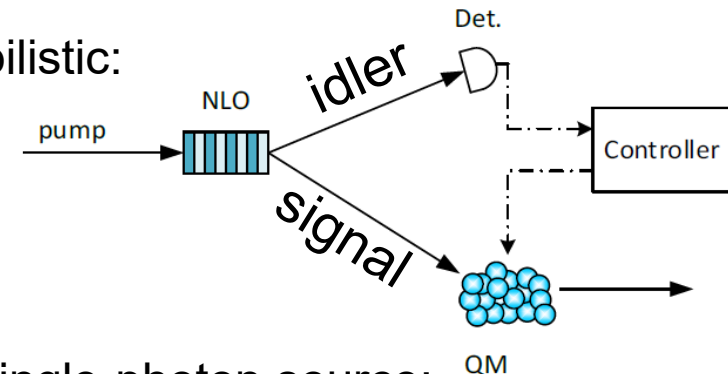


Fighting two problems of probabilistic creation of photons:

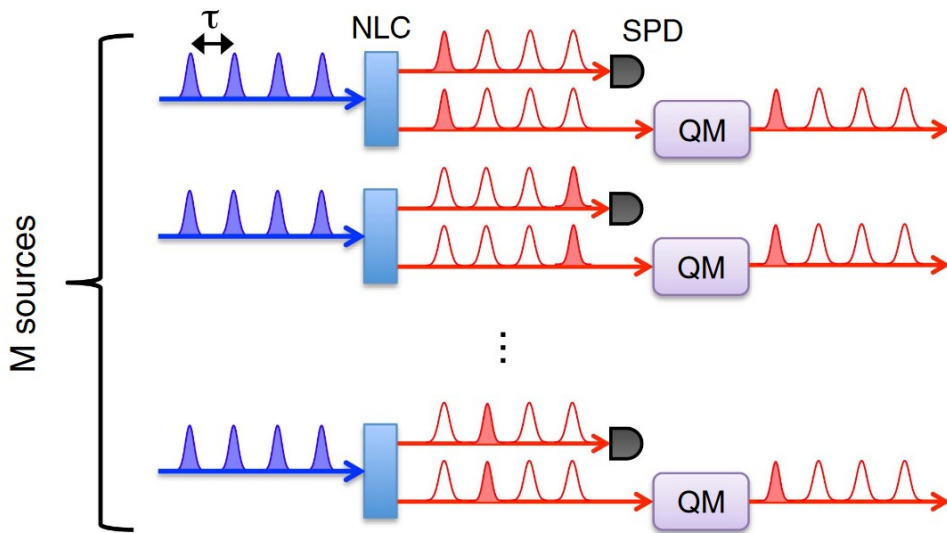
- photon number can be too low => long waiting times
- photon number too high results in creation of multiple pairs of photons.

# Applications – 1: QM-assisted multi-qubit states

- In the example, the creation of photons is probabilistic: spontaneous parametric down-conversion (SPDC); four-wave mixing (FWM);



- One photon of the pair is detected, heralding the arriving of the other one;
- Use quantum memory to create a deterministic single-photon source;
- Improves the performance of multi-channel experiments:



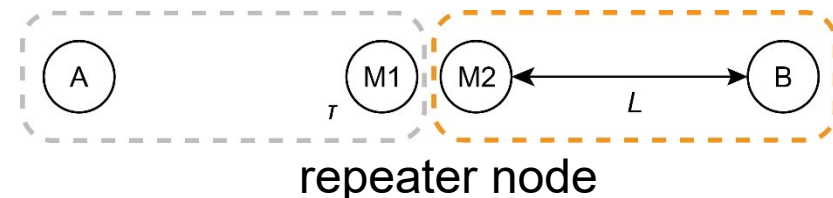
QKD rate enhancement of 250. Potential to get up to 30 single photons at Hz rates seems feasible, a 23-order-of-magnitude improvement over current state of the art.

$$p_1^M \text{ vs } p_1$$

$p_1$  – success probability per channel  
 $M$  – number of channels

## Applications – 2: Quantum repeater

A *quantum repeater* distributes the entanglement between the two remote nodes A and B, compensating for propagation loss and decoherence.



Challenges to overcome:

- attenuation / qubit loss ( $T_1$  – longitudinal relaxation time)
- decoherence / phase loss ( $T_2$  – transverse relaxation time)
- storing the other qubit – quantum memory

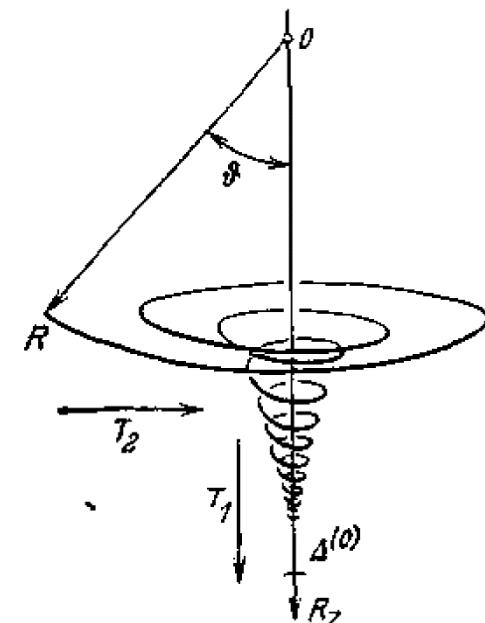
For a lossy channel:

memory lifetime  $\tau_m > (L/c) + \text{classical communication time}$

Fiber attenuation:  $\sim 1 \text{ dB/km}$

At  $L = 25 \text{ km}$ :  $\tau_m \sim 0.083 \text{ ms}$ ;  $T \sim 0.08 \Rightarrow 12 \text{ attempts (1 ms)}$

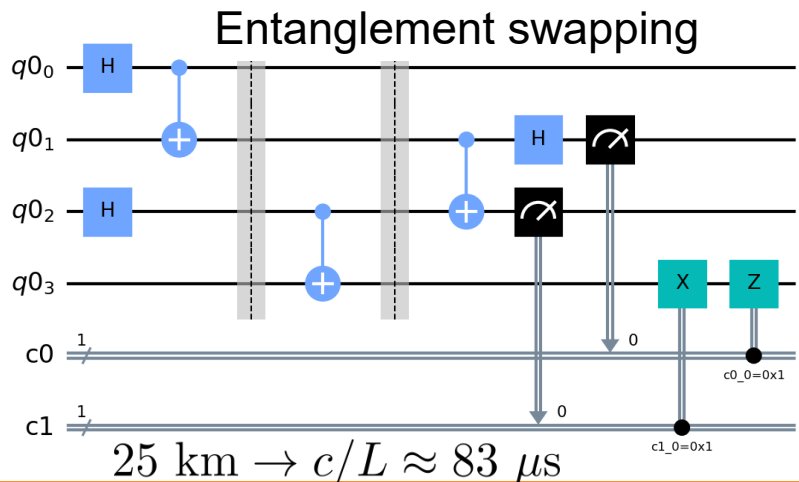
Duan, Lukin, Cirac, and Zoller (DLCZ) protocol.



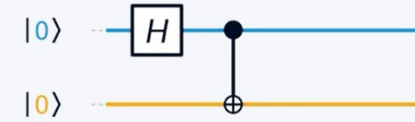
### Building blocks for a quantum repeater:

- Entanglement swapping
- Entanglement purification
- Repeater link architecture

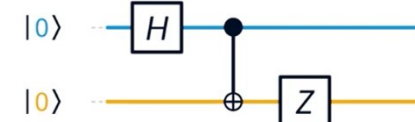
# Quantum repeater – 1: entanglement swapping



Bell state preparation...



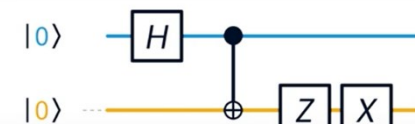
$$|\Phi_+\rangle = \frac{1}{\sqrt{2}} (|00\rangle + |11\rangle)$$



$$|\Phi_-\rangle = \frac{1}{\sqrt{2}} (|00\rangle - |11\rangle)$$



$$|\Psi_+\rangle = \frac{1}{\sqrt{2}} (|01\rangle + |10\rangle)$$



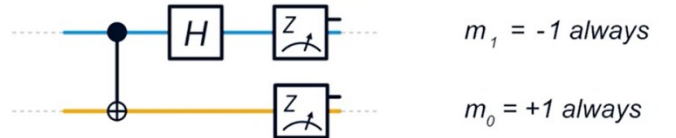
$$|\Psi_-\rangle = \frac{1}{\sqrt{2}} (|01\rangle - |10\rangle)$$

... and measurement:

$$|\Phi_+\rangle = \frac{1}{\sqrt{2}} (|00\rangle + |11\rangle)$$



$$|\Phi_-\rangle = \frac{1}{\sqrt{2}} (|00\rangle - |11\rangle)$$



$$|\Psi_+\rangle = \frac{1}{\sqrt{2}} (|01\rangle + |10\rangle)$$



$$|\Psi_-\rangle = \frac{1}{\sqrt{2}} (|01\rangle - |10\rangle)$$



## Quantum repeater – 2: entanglement purification

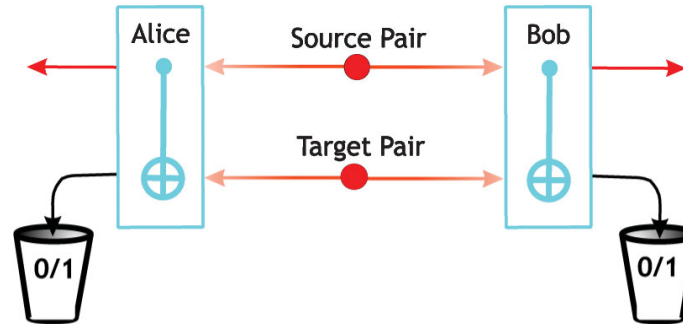
Start with a Bell state plus incoherent noise:

$$M = p |\Psi^-\rangle \langle \Psi^-| + (1 - p) \frac{|\Psi^+\rangle \langle \Psi^+| + |\Phi^-\rangle \langle \Phi^-| + |\Phi^+\rangle \langle \Phi^+|}{3}$$

Fidelity with respect to the initial state:  $F = \langle \Psi^- | M | \Psi^- \rangle$

Introducing a Werner state  $W_F$  of purity  $F$ :

$$W_F \equiv F |\Psi^-\rangle \langle \Psi^-| + \frac{1 - F}{3} |\Psi^-\rangle \langle \Psi^-| + \frac{1 - F}{3} |\Phi^+\rangle \langle \Phi^+| + \frac{1 - F}{3} |\Phi^-\rangle \langle \Phi^-|$$



[ C.H. Bennett et al., "Purification of Noisy Entanglement and Faithful Teleportation via Noisy Channels" // Phys. Rev. Lett. **76**, 722 (1996). <https://doi.org/10.1103/PhysRevLett.76.722> ]

## Quantum repeater – 2: entanglement purification

$$M = p |\Psi^-\rangle \langle \Psi^-| + (1-p) \frac{|\Psi^+\rangle \langle \Psi^+| + |\Phi^-\rangle \langle \Phi^-| + |\Phi^+\rangle \langle \Phi^+|}{3}$$

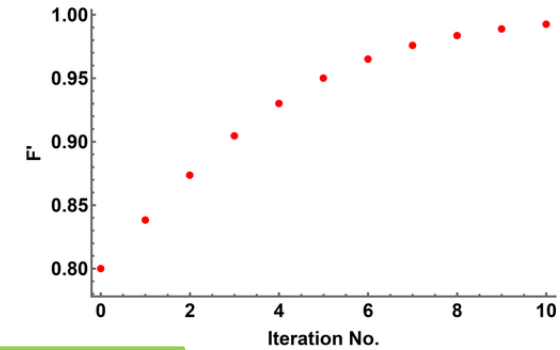
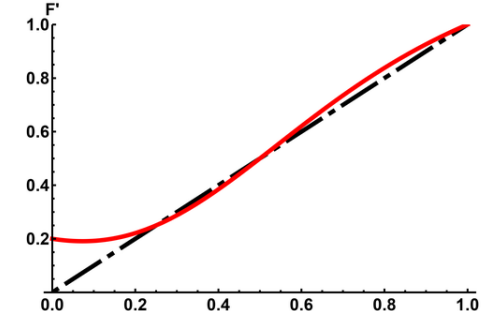
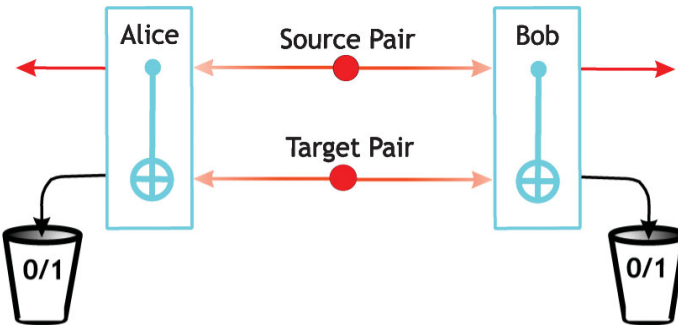
$$F = \langle \Psi^- | M | \Psi^- \rangle$$

Introducing a Werner state  $W_F$  of purity  $F$ :

$$W_F \equiv F |\Psi^-\rangle \langle \Psi^-| + \frac{1-F}{3} |\Psi^-\rangle \langle \Psi^-| + \frac{1-F}{3} |\Phi^+\rangle \langle \Phi^+| + \frac{1-F}{3} |\Phi^-\rangle \langle \Phi^-|$$

After performing the measurements and rejecting particular outcomes, we obtain a post-selected state  $W'$  with fidelity  $F'$ :

$$F' = \frac{F^2 + \frac{1}{9}(1-F)^2}{F^2 + \frac{2}{3}F(1-F) + \frac{5}{9}(1-F)^2}$$



[C.H. Bennett et al., "Purification of noisy entanglers," (1996). <https://doi.org/10.1103/PhysRevLett.76.722>

**Aalto University**  
[H.-J. Briegel, W. Dür, J. I. Cirac, "The Quantum repeater:peater – 2: entanglement purification", // Phys. Rev. Lett. 81 (26), 5932 (1998). <https://doi.org/10.1103/PhysRevLett.81.5932>]

□ Improve fidelity at the cost of sacrificing some of the Bell pairs.

vs. Rev. Lett. 76, 722

"Quantum Communication"

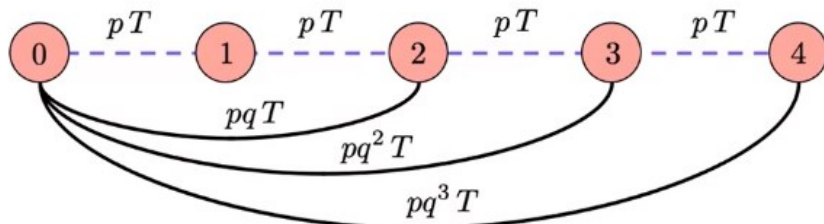
## Quantum repeater – 3: nested purification protocol

$T$  – time of establishing the entanglement link between the adjacent q. repeater nodes

$p$  – entanglement link generation probability

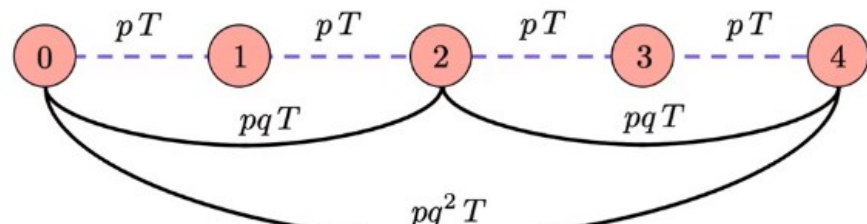
$q$  – entanglement swapping probability

**Sequential entanglement swapping:**



$$\propto pq^3$$

**Nested entanglement swapping:**



$$\propto pq^2$$

- Changing the protocol can significantly affect the resource cost.

# Applications – 2: Quantum repeater

PHYSICAL REVIEW LETTERS 130, 213601 (2023)

Editors' Suggestion

Featured in Physics

## Telecom-Wavelength Quantum Repeater Node Based on a Trapped-Ion Processor

V. Krutyanskiy<sup>1,2</sup>, M. Canteri<sup>1,2</sup>, M. Meraner<sup>1,2</sup>, J. Bate<sup>1,2</sup>, V. Kremarsky<sup>2,1</sup>, J. Schupp<sup>1,2</sup>, N. Sangouard<sup>3</sup>, and B. P. Lanyon<sup>1,2,\*</sup>

<sup>1</sup>Institut für Experimentalphysik, Universität Innsbruck, Technikerstrasse 25, 6020 Innsbruck, Austria

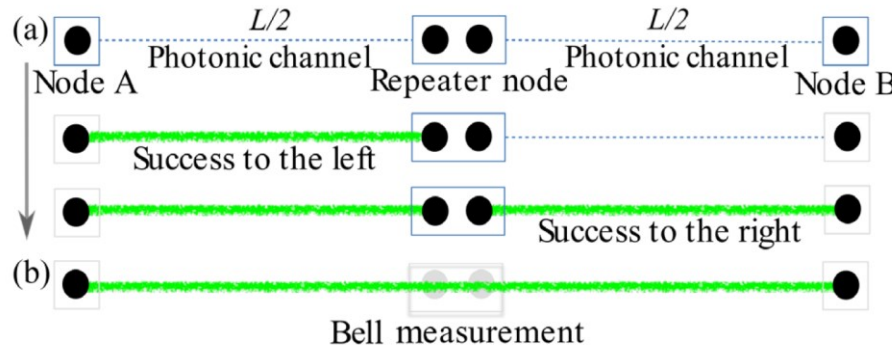
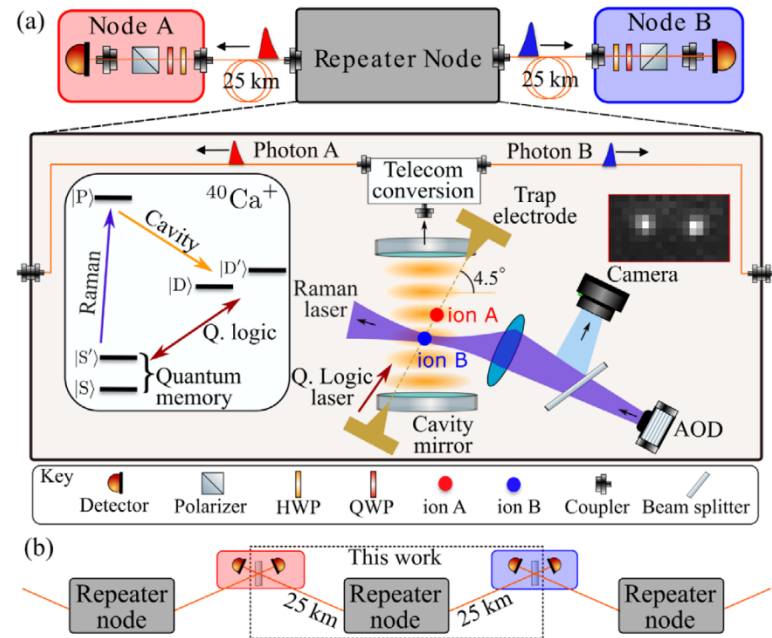
<sup>2</sup>Institut für Quantenoptik und Quanteninformation, Österreichische Akademie der Wissenschaften, Technikerstrasse 21a, 6020 Innsbruck, Austria

<sup>3</sup>Institut de Physique Théorique, Université Paris-Saclay, CEA, CNRS, 91191 Gif-sur-Yvette, France

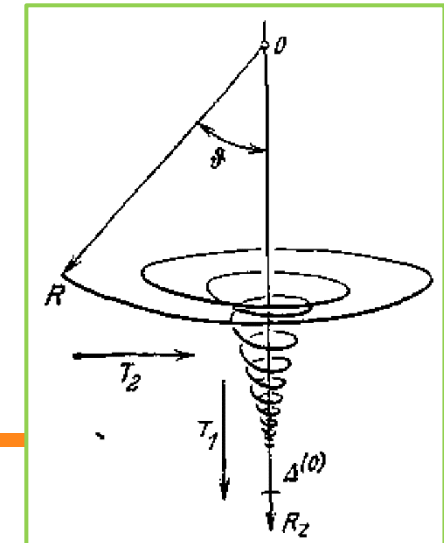
(Received 19 October 2022; revised 17 February 2023; accepted 16 March 2023; published 22 May 2023)

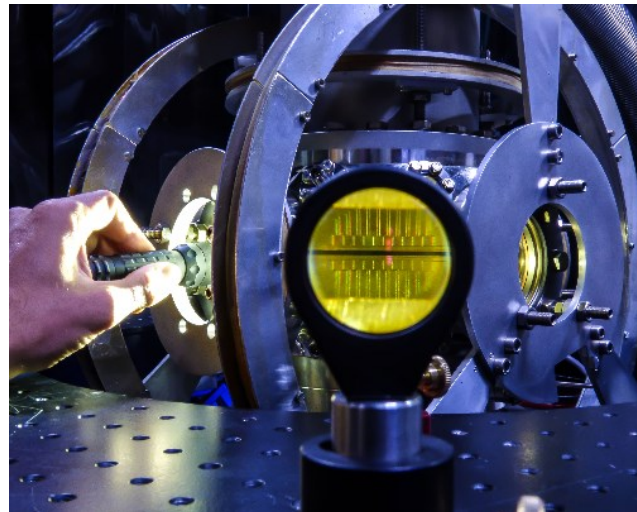
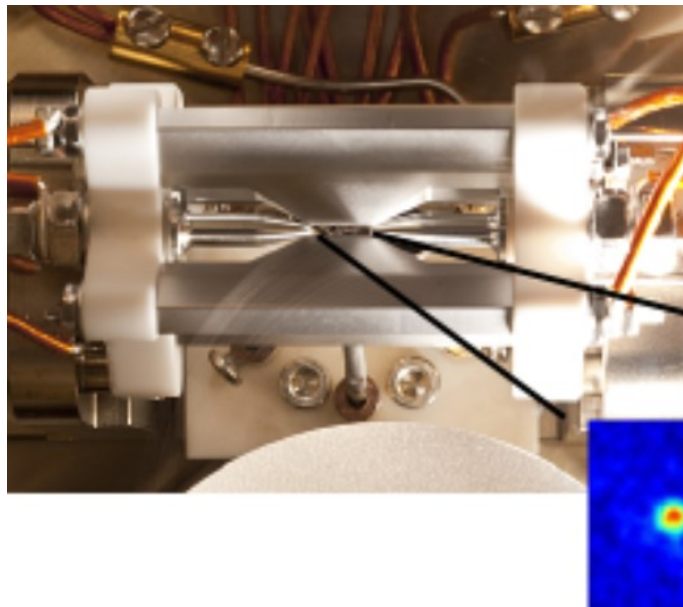
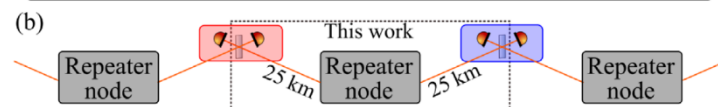
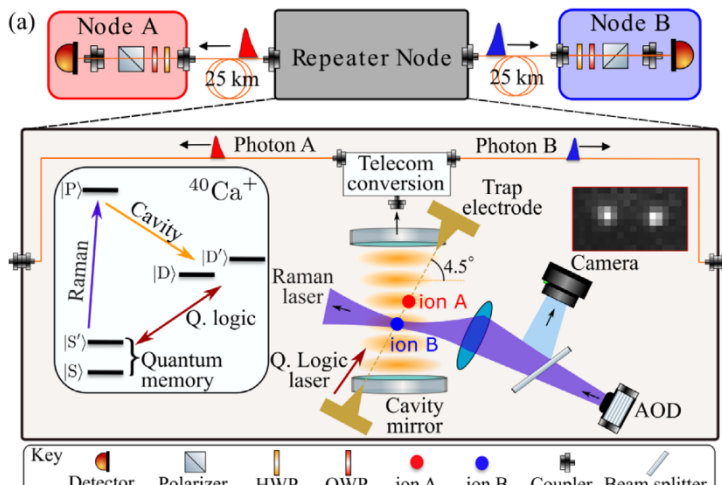
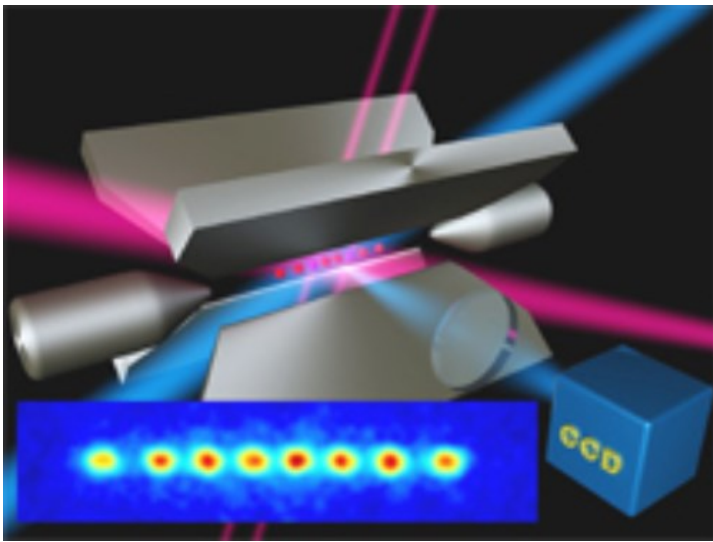
A quantum repeater node is presented based on trapped ions that act as single-photon emitters, quantum memories, and an elementary quantum processor. The node's ability to establish entanglement across two 25-km-long optical fibers independently, then to swap that entanglement efficiently to extend it over both fibers, is demonstrated. The resultant entanglement is established between telecom-wavelength photons at either end of the 50 km channel. Finally, the system improvements to allow for repeater-node chains to establish stored entanglement over 800 km at hertz rates are calculated, revealing a near-term path to distributed networks of entangled sensors, atomic clocks, and quantum processors.

DOI: 10.1103/PhysRevLett.130.213601



[ V. Krutyanskiy et al., “Telecom-Wavelength Quantum Repeater Node Based on a Trapped-Ion Processor” // Phys. Rev. Lett. 130, 213601 (2023).  
<https://doi.org/10.1103/PhysRevLett.130.213601> ]



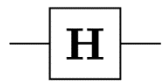


## The layout of an ion trap – quantum memory for a quantum repeater.

[ University of Innsbruck, Quantum optics & spectroscopy group,  
<https://www.quantumoptics.at/en/research.html> ]

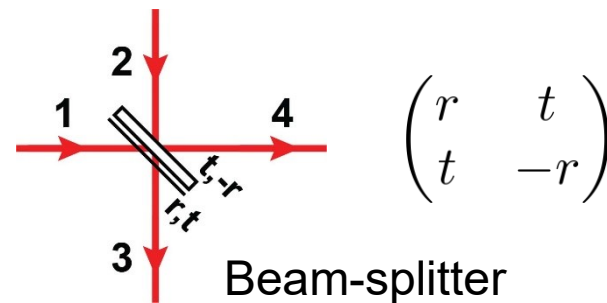
[ V. Krutyanskiy *et al.*, "Telecom-Wavelength Quantum Repeater Node Based on a Trapped-Ion Processor" // *Phys. Rev. Lett.* **130**, 213601 (2023).  
<https://doi.org/10.1103/PhysRevLett.130.213601> ]

# Applications of Quantum Optics



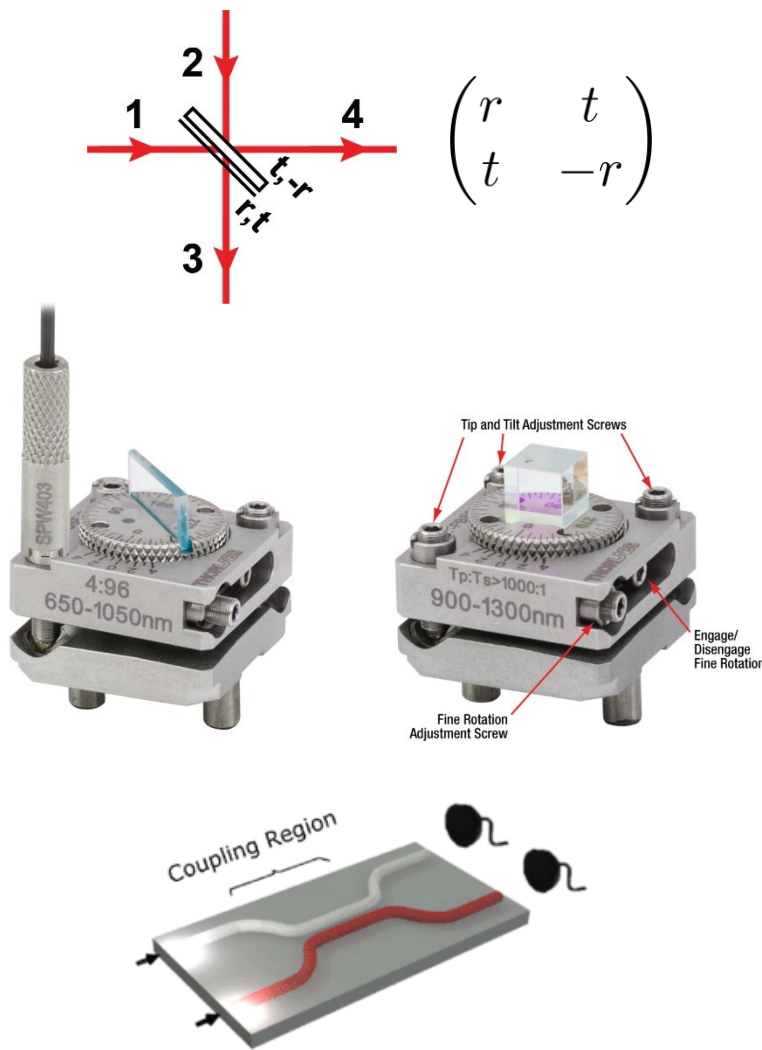
$$\frac{1}{\sqrt{2}} \begin{bmatrix} 1 & 1 \\ 1 & -1 \end{bmatrix}$$

Hadamard gate



- Beam-splitter transfer matrix
- Field operator transformation for a beam-splitter
- Calculating the output field state
- Hong-Ou-Mandel interference
- Mach-Zehnder Interferometer

# Beam splitter



- Path-encoded qubits:

$$|“0”\rangle = |1\rangle_1 \otimes |0\rangle_2 = |1\rangle_1 |0\rangle_2$$

$$|“1”\rangle = |0\rangle_1 \otimes |1\rangle_2 = |0\rangle_1 |1\rangle_2$$

- Loss-less  $\Rightarrow$  unitary transformation  
(can be generalized to a lossy one)

$$|r|^2 = R, |t|^2 = T, R + T = 1$$

$r, t$  – amplitude coefficients

$R, T$  – power (= intensity) coefficients

# General statements on the single-mode quantized radiation

We are working with an idealized system of a single-mode quantized radiation. “Mode”  $l$  here stands for both polarization  $\mathbf{e}_l$  and propagation direction  $\mathbf{k}_l$ .

$$\hat{\mathcal{H}} = \hbar\omega_l \left( \hat{a}_l^\dagger \hat{a}_l + \frac{1}{2} \right)$$

$$\hat{\mathbf{E}}_l(\mathbf{r}) = i\mathbf{e}_l \xi_l^{(1)} \left( \hat{a}_l e^{+i\mathbf{k}_l \cdot \mathbf{r}} - \hat{a}_l^\dagger e^{-i\mathbf{k}_l \cdot \mathbf{r}} \right)$$

(Note the Heisenberg picture.)

$|n\rangle_l$  — number state = Fock state

Number of photons in mode “ $l$ ” is fixed to  $n$ .

$\hat{n}_l \equiv \hat{a}_l^\dagger \hat{a}_l$  — operator for the number of photons in the mode “ $l$ ”.

$\xi_l^{(1)} = \sqrt{\frac{\hbar\omega_l}{2\epsilon_0 V_l}}$  — one-photon [field] amplitude.

Photon creation ( $\hat{a}$ ) and annihilation ( $\hat{a}^\dagger$ ) operators for light in mode  $l$ :

$$\begin{aligned} [\hat{a}_p; \hat{a}_q] &= 0, [\hat{a}_p^\dagger; \hat{a}_q^\dagger] = 0, \\ [\hat{a}_p; \hat{a}_q^\dagger] &\equiv \hat{a}_p \hat{a}_q^\dagger - \hat{a}_q^\dagger \hat{a}_p^\dagger = \delta_{pq} = \\ &= \begin{cases} 1, & p = q \\ 0, & p \neq q \end{cases} \end{aligned}$$

Introduced in the field quantization,  
e.g. GAF'2010 Sec. 4.

Useful relations:

$$\hat{a} |n\rangle_F = \sqrt{n} |n-1\rangle_F$$

$$\hat{a}^\dagger |n-1\rangle_F = \sqrt{n} |n\rangle_F$$

$$\hat{n} |n\rangle_F \equiv \hat{a}^\dagger \hat{a} |n\rangle_F = n |n\rangle_F$$

$$\hat{a} |0\rangle = 0 \cdot |0\rangle = 0$$

# General statements on the single-mode quantized radiation

$$\hat{\mathcal{H}} = \hbar\omega_l \left( \hat{a}_l^\dagger \hat{a}_l + \frac{1}{2} \right)$$

$$\hat{\mathbf{E}}_l(\mathbf{r}) = i\mathbf{e}_l \xi_l^{(1)} \left( \hat{a}_l e^{i\mathbf{k}_l \cdot \mathbf{r}} - \hat{a}_l^\dagger e^{-i\mathbf{k}_l \cdot \mathbf{r}} \right)$$

$|n\rangle_l$  — number state = Fock state

Number of photons in mode “*l*” is fixed to *n*.

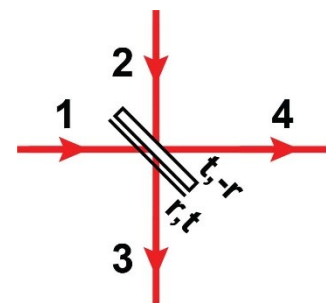
$$\hat{\mathbf{E}}_l^{(+)}(\mathbf{r}) = +i\mathbf{e}_l \xi_l^{(1)} \hat{a}_l e^{i\mathbf{k}_l \cdot \mathbf{r}}$$

analytic signal, or  
positive frequency part

$$\hat{\mathbf{E}}_l^{(-)}(\mathbf{r}) = -i\mathbf{e}_l \xi_l^{(1)} \hat{a}_l^\dagger e^{-i\mathbf{k}_l \cdot \mathbf{r}} = \text{h.c.} \left\{ \hat{\mathbf{E}}_l^{(+)} \right\}$$

Classical radiation:

$$\begin{pmatrix} \mathbf{E}_3^{(+)}(\mathbf{r}) \\ \mathbf{E}_4^{(+)}(\mathbf{r}) \end{pmatrix} = \begin{pmatrix} r & t \\ t & -r \end{pmatrix} \begin{pmatrix} \mathbf{E}_1^{(+)}(\mathbf{r}) \\ \mathbf{E}_2^{(+)}(\mathbf{r}) \end{pmatrix}$$



“Quantized light:

$$\begin{pmatrix} \hat{\mathbf{E}}_3^{(+)}(\mathbf{r}) \\ \hat{\mathbf{E}}_4^{(+)}(\mathbf{r}) \end{pmatrix} = \begin{pmatrix} r & t \\ t & -r \end{pmatrix} \begin{pmatrix} \hat{\mathbf{E}}_1^{(+)}(\mathbf{r}) \\ \hat{\mathbf{E}}_2^{(+)}(\mathbf{r}) \end{pmatrix}$$

Photon creation ( $\hat{a}$ ) and annihilation ( $\hat{a}^\dagger$ ) operators for light in mode *l*:

$$[\hat{a}_p; \hat{a}_q] = 0, [\hat{a}_p^\dagger; \hat{a}_q^\dagger] = 0,$$

$$[\hat{a}_p; \hat{a}_q^\dagger] \equiv \hat{a}_p \hat{a}_q^\dagger - \hat{a}_q^\dagger \hat{a}_p^\dagger = \delta_{pq} =$$

$$= \begin{cases} 1, & p = q \\ 0, & p \neq q \end{cases}$$

Introduced in the field quantization,  
e.g. GAF'2010 Sec. 4.

Useful relations:

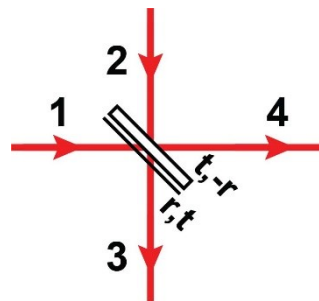
$$\hat{a} |n\rangle_F = \sqrt{n} |n-1\rangle_F$$

$$\hat{a}^\dagger |n-1\rangle_F = \sqrt{n} |n\rangle_F$$

$$\hat{n} |n\rangle_F \equiv \hat{a}^\dagger \hat{a} |n\rangle_F = n |n\rangle_F$$

$$\hat{a} |0\rangle = 0 \cdot |0\rangle = 0$$

# Beam-splitter + classical radiation



$$\begin{pmatrix} \mathbf{E}_3^{(+)}(\mathbf{r}) \\ \mathbf{E}_4^{(+)}(\mathbf{r}) \end{pmatrix} = \begin{pmatrix} r & t \\ t & -r \end{pmatrix} \begin{pmatrix} \mathbf{E}_1^{(+)}(\mathbf{r}) \\ \mathbf{E}_2^{(+)}(\mathbf{r}) \end{pmatrix}$$

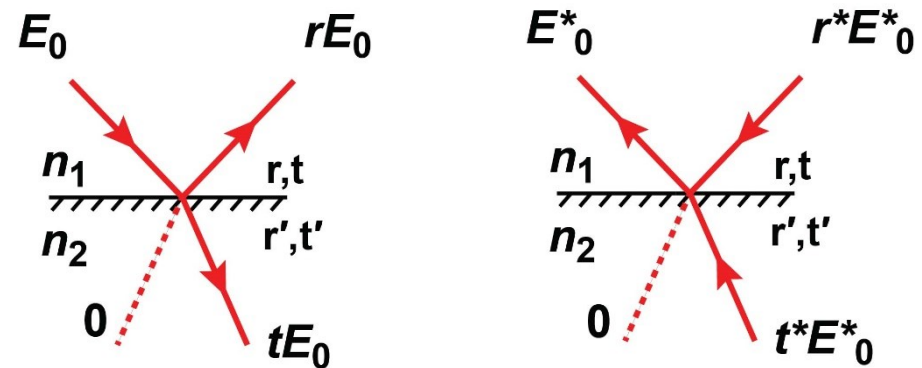
- Why the sign?

→ time-reversal symmetry  
(Helmholtz reciprocity principle)

$$\mathbf{E}_l(\mathbf{r}) \sim E_0 e^{-i\omega t + i\mathbf{k}_l \cdot \mathbf{r}} + \text{c.c.}$$

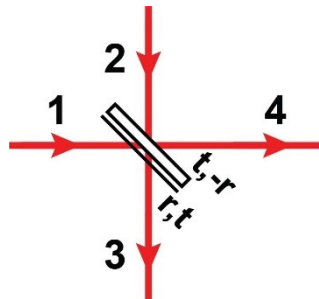
$$\mathbf{k}_l \rightarrow -\mathbf{k}_l, t \rightarrow -t: (\mathbf{E}_l(\mathbf{r}))^*$$

- Orientation (“ $-r$ ”) is marked with an additional line.



$$\begin{cases} r^*r + t^*t' = 1 \\ r^*t + t^*r' = 0 \\ |r|^2 + |t|^2 = 1 \\ |r'|^2 + |t'|^2 = 1 \end{cases} \rightarrow \begin{cases} t = t' \in \mathbb{R} \\ r^* = -r' \end{cases}$$

# Beam-splitter + quantized radiation



$$\begin{pmatrix} \hat{\mathbf{E}}_3^{(+)}(\mathbf{r}) \\ \hat{\mathbf{E}}_4^{(+)}(\mathbf{r}) \end{pmatrix} = \begin{pmatrix} r & t \\ t & -r \end{pmatrix} \begin{pmatrix} \hat{\mathbf{E}}_1^{(+)}(\mathbf{r}) \\ \hat{\mathbf{E}}_2^{(+)}(\mathbf{r}) \end{pmatrix}$$

General case:

output field operators are the linear transformation of the input field operators.

$$\begin{pmatrix} \hat{a}_3 \\ \hat{a}_4 \end{pmatrix} = \hat{U} \begin{pmatrix} \hat{a}_1 \\ \hat{a}_2 \end{pmatrix} \hat{U}^\dagger \quad \begin{pmatrix} \hat{a}_3^\dagger \\ \hat{a}_4^\dagger \end{pmatrix} = M \begin{pmatrix} \hat{a}_1^\dagger \\ \hat{a}_2^\dagger \end{pmatrix} = \begin{pmatrix} r_1 & t_1 \\ t_2 & r_2 \end{pmatrix} \begin{pmatrix} \hat{a}_1^\dagger \\ \hat{a}_2^\dagger \end{pmatrix}$$

$\hat{U}$  – must be unitary;  $M$  – not necessarily.

For the output field operators to be physically meaningful, they should respect the commutation relations → can calculate  $r, t, r'$ , and  $t'$  coefficients:

$$[\hat{a}_1; \hat{a}_1] = 0, [\hat{a}_1^\dagger; \hat{a}_1^\dagger] = 0, [\%]_2, \quad [\hat{a}_3; \hat{a}_3] = 0, [\hat{a}_3^\dagger; \hat{a}_3^\dagger] = 0, [\%]_4,$$

$$[\hat{a}_1; \hat{a}_1^\dagger] \equiv \hat{a}_1 \hat{a}_1^\dagger - \hat{a}_1^\dagger \hat{a}_1^\dagger = 1, [\%]_2 \quad [\hat{a}_3; \hat{a}_3^\dagger] \equiv \hat{a}_3 \hat{a}_3^\dagger - \hat{a}_3^\dagger \hat{a}_3^\dagger = 1, [\%]_4$$

## Beam-splitter + quantized radiation

(Operator hats are omitted.)

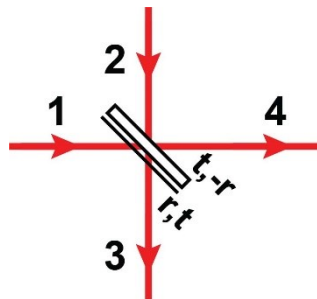
$$\begin{aligned} [a_3; a_3^\dagger] &\equiv a_3 a_3^\dagger - a_3^\dagger a_3 = \\ &= (r_1^* a_1 + t_1^* a_2) (r_1 a_1^\dagger + t_1 a_2^\dagger) - (r_1 a_1^\dagger + t_1 a_2^\dagger) (r_1^* a_1 + t_1^* a_2) = \\ &= |r_1|^2 a_1 a_1^\dagger + r_1^* t_1 a_1 a_2^\dagger + t_1^* r_1 a_2 a_1^\dagger + |t_1|^2 a_2 a_2^\dagger - \\ &- |r_1|^2 a_1^\dagger a_1 - r_1 t_1^* a_1^\dagger a_2 - t_1 r_1^* a_2^\dagger a_1 - |t_1|^2 a_2^\dagger a_2 \end{aligned}$$

Different modes do not commute:

$$[a_1; a_2^\dagger] = 0 \Rightarrow a_1 a_2^\dagger = a_2^\dagger a_1 \quad [a_3; a_3^\dagger] = |r_1|^2 + |t_1|^2 = 1$$

$$\begin{aligned} [a_3; a_4^\dagger] &\equiv a_3 a_4^\dagger - a_4^\dagger a_3 = \\ &= (r_1^* a_1 + t_1^* a_2) (t_2 a_1^\dagger + r_2 a_2^\dagger) - (t_2 a_1^\dagger + r_2 a_2^\dagger) (r_1^* a_1 + t_1^* a_2) = \\ &= r_1^* t_2 a_1 a_1^\dagger + r_1^* r_2 a_1 a_2^\dagger + t_1^* t_2 a_2 a_1^\dagger + r_2 t_1^* a_2 a_2^\dagger - \\ &- r_1^* t_2 a_1^\dagger a_1 - t_1^* t_2 a_1^\dagger a_2 - r_2^* t_1 a_2^\dagger a_2 - r_2 r_1^* a_2^\dagger a_1 = \quad [a_3; a_4^\dagger] = r_1^* t_2 + r_2 t_1^* = 0 \\ &= r_1^* t_2 + r_2 t_1^* + 0 + 0 \end{aligned}$$

# Beam-splitter transfer matrix



$$\begin{pmatrix} \hat{a}_3^\dagger \\ \hat{a}_4^\dagger \end{pmatrix} = M \begin{pmatrix} \hat{a}_1^\dagger \\ \hat{a}_2^\dagger \end{pmatrix} = \begin{pmatrix} r_1 & t_1 \\ t_2 & r_2 \end{pmatrix} \begin{pmatrix} \hat{a}_1^\dagger \\ \hat{a}_2^\dagger \end{pmatrix} \quad |r|^2 + |t|^2 = 1$$
$$r_1^* t_2 + r_2 t_1^* = 0$$

There are a few commonly used transfer matrices satisfying the above conditions:

“real”:  $M = \begin{pmatrix} r & t \\ t & -r \end{pmatrix}$

“symmetric”:  $M = \begin{pmatrix} r & it \\ it & r \end{pmatrix}$

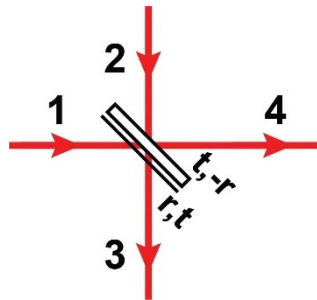
“general”:  $M = e^{+i\Lambda/2} \begin{pmatrix} \cos\left(\frac{\theta}{2}\right) e^{+i(\psi+\phi)/2} & \sin\left(\frac{\theta}{2}\right) e^{+i(\psi-\phi)/2} \\ -\sin\left(\frac{\theta}{2}\right) e^{-i(\psi-\phi)/2} & \cos\left(\frac{\theta}{2}\right) e^{-i(\psi+\phi)/2} \end{pmatrix}$

In all cases, the coefficients are real numbers.

The form of the matrix can only be chosen once.

- ❖ Is  $M$  a unitary matrix?
- ❖ **Reversed transformation:**  
Express  $\hat{a}_1^\dagger$  and  $\hat{a}_2^\dagger$  through  $\hat{a}_3^\dagger$  and  $\hat{a}_4^\dagger$ ?

# Beam-splitter transfer matrix



$$\begin{pmatrix} \hat{a}_3^\dagger \\ \hat{a}_4^\dagger \end{pmatrix} = M \begin{pmatrix} \hat{a}_1^\dagger \\ \hat{a}_2^\dagger \end{pmatrix} = \begin{pmatrix} r_1 & t_1 \\ t_2 & r_2 \end{pmatrix} \begin{pmatrix} \hat{a}_1^\dagger \\ \hat{a}_2^\dagger \end{pmatrix} \quad |r|^2 + |t|^2 = 1$$

$$r_1^* t_2 + r_2 t_1^* = 0$$

There are a few commonly used transfer matrices satisfying the above conditions:

“real”:  $M = \begin{pmatrix} r & t \\ t & -r \end{pmatrix}$

“symmetric”:  $M = \begin{pmatrix} r & it \\ it & r \end{pmatrix}$

“general”:  $M = e^{+i\Lambda/2} \begin{pmatrix} \cos\left(\frac{\theta}{2}\right) e^{+i(\psi+\phi)/2} & \sin\left(\frac{\theta}{2}\right) e^{+i(\psi-\phi)/2} \\ -\sin\left(\frac{\theta}{2}\right) e^{-i(\psi-\phi)/2} & \cos\left(\frac{\theta}{2}\right) e^{-i(\psi+\phi)/2} \end{pmatrix}$

In all cases, the coefficients are real numbers.

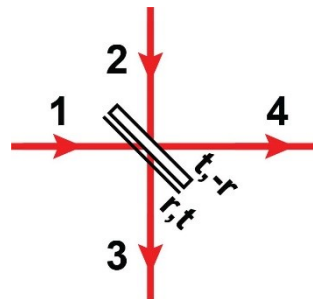
The form of the matrix can only be chosen once.

- ❖ Is  $M$  a unitary matrix?
- ❖ **Reversed transformation:**  
Express  $\hat{a}_1^\dagger$  and  $\hat{a}_2^\dagger$  through  $\hat{a}_3^\dagger$  and  $\hat{a}_4^\dagger$ ?

$$\begin{pmatrix} \hat{a}_1^\dagger \\ \hat{a}_2^\dagger \end{pmatrix} = \frac{1}{r_1 r_2 - t_1 t_2} \begin{pmatrix} r_2^* & -t_2^* \\ -t_1^* & r_1^* \end{pmatrix} \begin{pmatrix} \hat{a}_3^\dagger \\ \hat{a}_4^\dagger \end{pmatrix}$$

e.g.  $\begin{pmatrix} r & t \\ t & -r \end{pmatrix}$

## Beam-splitter



From now on, we will be using the real form of the transfer matrix:

$$\begin{pmatrix} \hat{a}_3^\dagger \\ \hat{a}_4^\dagger \end{pmatrix} = \begin{pmatrix} r & t \\ t & -r \end{pmatrix} \begin{pmatrix} \hat{a}_1^\dagger \\ \hat{a}_2^\dagger \end{pmatrix}, \quad \begin{pmatrix} \hat{a}_1^\dagger \\ \hat{a}_2^\dagger \end{pmatrix} = \begin{pmatrix} r & t \\ t & -r \end{pmatrix} \begin{pmatrix} \hat{a}_3^\dagger \\ \hat{a}_4^\dagger \end{pmatrix}$$

A beam-splitter can thus be considered an implementation of a Hadamard gate:  $\begin{pmatrix} r & t \\ t & -r \end{pmatrix} \Big|_{r=t=1/\sqrt{2}} \rightarrow \frac{1}{\sqrt{2}} \begin{pmatrix} 1 & 1 \\ 1 & -1 \end{pmatrix}$

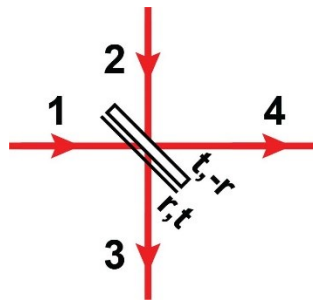
The formalism is used for calculating expectation values and output states.

$$\langle \Psi_{out} | \hat{B}_{out} | \Psi_{out} \rangle = \langle \Psi_{out} | U^\dagger U \hat{B}_{out} U^\dagger U | \Psi_{out} \rangle = \langle \Psi_{in} | \hat{B}_{in} | \Psi_{in} \rangle$$

Two approaches:

- Express output operators through the input ones + compute observables
- Convert input state to the output state.

## A. Converting operators (output to input)



Example: Hong-Ou-Mandel interference

Single detection probability  $P$  :

$$\frac{dP}{dt} = \int_{S_{det}, T_{det}} w^{(1)}(\mathbf{r}, t) dS dt$$

$$w^{(1)}(\mathbf{r}, t) = s \langle \Psi(t) | \hat{\mathbf{E}}^{(-)}(\mathbf{r}) \hat{\mathbf{E}}^{(+)}(\mathbf{r}) | \Psi(t) \rangle$$

$$w^{(1)}(\mathbf{r}, t) \sim |\hat{a}^\dagger \hat{a} | \Psi(t) \rangle|^2$$

Double detections:

$$\frac{dP}{dt} = \int_{S_{det}, T_{det}} w^{(2)}(\mathbf{r}, t, \mathbf{r}', t') dS dS' dt dt'$$

$$w^{(2)}(\mathbf{r}, t, \mathbf{r}', t') = s^2 \langle \Psi(t) | \hat{\mathbf{E}}^{(-)}(\mathbf{r}) \hat{\mathbf{E}}^{(-)}(\mathbf{r}') \hat{\mathbf{E}}^{(+)}(\mathbf{r}) \hat{\mathbf{E}}^{(+)}(\mathbf{r}') | \Psi(t) \rangle$$

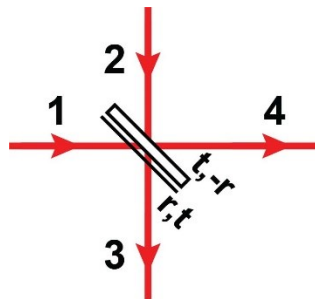
$$w^{(2)}(\mathbf{r}, t, \mathbf{r}', t') \sim |\hat{a}^\dagger(\mathbf{r}) \hat{a}^\dagger(\mathbf{r}') \hat{a}(\mathbf{r}) \hat{a}(\mathbf{r}') | \Psi(t) \rangle|^2$$

$w^{(2)} \neq (w^{(1)})^2$  : measuring the state with one detector changes the state of the system.

$$\hat{\mathbf{E}}_l^{(+)}(\mathbf{r}) = +i\mathbf{e}_l \xi_l^{(1)} \hat{a}_l e^{+i\mathbf{k}_l \mathbf{r}}$$

$$\hat{\mathbf{E}}_l^{(-)}(\mathbf{r}) = -i\mathbf{e}_l \xi_l^{(1)} \hat{a}_l^\dagger e^{-i\mathbf{k}_l \mathbf{r}} = \text{h.c.} \left\{ \hat{\mathbf{E}}_l^{(+)} \right\}$$

## A. Converting operators (output to input)



Example: Hong-Ou-Mandel interference

$$\begin{pmatrix} \hat{a}_3^\dagger \\ \hat{a}_4^\dagger \end{pmatrix} = \begin{pmatrix} r & t \\ t & -r \end{pmatrix} \begin{pmatrix} \hat{a}_1^\dagger \\ \hat{a}_2^\dagger \end{pmatrix}, \quad \begin{pmatrix} \hat{a}_1^\dagger \\ \hat{a}_2^\dagger \end{pmatrix} = \begin{pmatrix} r & t \\ t & -r \end{pmatrix} \begin{pmatrix} \hat{a}_3^\dagger \\ \hat{a}_4^\dagger \end{pmatrix}$$

1. Number of photons at the output for a single-photon input:  $|\Psi_{in}\rangle = |1\rangle_1 |0\rangle_2$

$$\langle \Psi_{out} | \hat{a}_3^\dagger \hat{a}_3 | \Psi_{out} \rangle = \langle \Psi_{in} | (r\hat{a}_1^\dagger + t\hat{a}_2^\dagger) (r\hat{a}_1 + t\hat{a}_2) | \Psi_{in} \rangle \rightarrow \\ \rightarrow \langle 1|_1 \langle 0|_2 (r\hat{a}_1^\dagger + t\hat{a}_2^\dagger) (r\hat{a}_1 + t\hat{a}_2) |1\rangle_1 |0\rangle_2 = (r\sqrt{1} \langle 0|_1 \langle 0|_2 + 0) (r\sqrt{1} |0\rangle_1 |0\rangle_2 + 0) = r^2$$

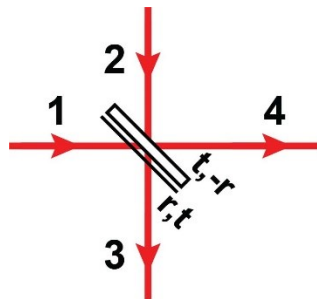
2. Coincidences for a biphoton input:  $|\Psi_{in}\rangle = |1\rangle_1 |1\rangle_2$

$$\langle \Psi_{out} | \hat{a}_3^\dagger \hat{a}_4^\dagger \hat{a}_3 \hat{a}_4 | \Psi_{out} \rangle \rightarrow$$

❖ ...

$w^{(1)} \sim  \hat{a}^\dagger \hat{a}  \Psi(t)\rangle ^2$	$\hat{a}_l  n\rangle_l = \sqrt{n}  n-1\rangle$
$w^{(2)} \sim  \hat{a}_1^\dagger \hat{a}_2^\dagger \hat{a}_1 \hat{a}_2  \Psi(t)\rangle ^2$	$\hat{a}_l^\dagger  n-1\rangle_l = \sqrt{n}  n\rangle$

## A. Converting operators (output to input)



Example: Hong-Ou-Mandel interference

$$\begin{pmatrix} \hat{a}_3^\dagger \\ \hat{a}_4^\dagger \end{pmatrix} = \begin{pmatrix} r & t \\ t & -r \end{pmatrix} \begin{pmatrix} \hat{a}_1^\dagger \\ \hat{a}_2^\dagger \end{pmatrix}, \quad \begin{pmatrix} \hat{a}_1^\dagger \\ \hat{a}_2^\dagger \end{pmatrix} = \begin{pmatrix} r & t \\ t & -r \end{pmatrix} \begin{pmatrix} \hat{a}_3^\dagger \\ \hat{a}_4^\dagger \end{pmatrix}$$

1. Number of photons at the output for a single-photon input:  $|\Psi_{in}\rangle = |1\rangle_1 |0\rangle_2$

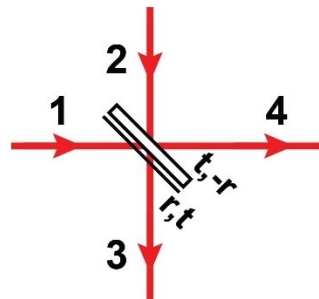
$$\langle \Psi_{out} | \hat{a}_3^\dagger \hat{a}_3 | \Psi_{out} \rangle = \langle \Psi_{in} | (r\hat{a}_1^\dagger + t\hat{a}_2^\dagger) (r\hat{a}_1 + t\hat{a}_2) | \Psi_{in} \rangle \rightarrow \\ \rightarrow \langle 1|_1 \langle 0|_2 (r\hat{a}_1^\dagger + t\hat{a}_2^\dagger) (r\hat{a}_1 + t\hat{a}_2) |1\rangle_1 |0\rangle_2 = (r\sqrt{1} \langle 0|_1 \langle 0|_2 + 0) (r\sqrt{1} |0\rangle_1 |0\rangle_2 + 0) = r^2$$

2. Coincidences for a biphoton input:  $|\Psi_{in}\rangle = |1\rangle_1 |1\rangle_2$

$$\langle \Psi_{out} | \hat{a}_3^\dagger \hat{a}_4^\dagger \hat{a}_3 \hat{a}_4 | \Psi_{out} \rangle \rightarrow \langle 1|_1 \langle 1|_2 (r\hat{a}_1^\dagger + t\hat{a}_2^\dagger) (t\hat{a}_1^\dagger - r\hat{a}_2^\dagger) (r\hat{a}_1 + t\hat{a}_2) (t\hat{a}_1 - r\hat{a}_2) |1\rangle_1 |1\rangle_2 \rightarrow \\ \rightarrow \langle 0|_1 \langle 0|_2 (0 - \sqrt{1}\sqrt{1}r^2 + \sqrt{1}\sqrt{1}t^2 - 0) (0 - r^2\sqrt{1}\sqrt{1} + t^2\sqrt{1}\sqrt{1} - 0) |0\rangle_1 |0\rangle_2 = \\ = (t^2 - r^2)^2 = 0 \quad \text{if } r = t = 1/\sqrt{2}$$

$w^{(1)} \sim  \hat{a}^\dagger \hat{a}  \Psi(t)\rangle ^2$	$\hat{a}_l  n\rangle_l = \sqrt{n}  n-1\rangle$
$w^{(2)} \sim  \hat{a}_1^\dagger \hat{a}_2^\dagger \hat{a}_1 \hat{a}_2  \Psi(t)\rangle ^2$	$\hat{a}_l^\dagger  n-1\rangle_l = \sqrt{n}  n\rangle$

## A. Converting operators (output to input)



Example: Hong-Ou-Mandel interference

$$\begin{pmatrix} \hat{a}_3^\dagger \\ \hat{a}_4^\dagger \end{pmatrix} = \begin{pmatrix} r & t \\ t & -r \end{pmatrix} \begin{pmatrix} \hat{a}_1^\dagger \\ \hat{a}_2^\dagger \end{pmatrix}, \quad \begin{pmatrix} \hat{a}_1^\dagger \\ \hat{a}_2^\dagger \end{pmatrix} = \begin{pmatrix} r & t \\ t & -r \end{pmatrix} \begin{pmatrix} \hat{a}_3^\dagger \\ \hat{a}_4^\dagger \end{pmatrix}$$

1. Number of photons at the output for a single-photon input:  $|\Psi_{in}\rangle = |1\rangle_1 |0\rangle_2$

$$\langle \Psi_{out} | \hat{a}_3^\dagger \hat{a}_3 | \Psi_{out} \rangle = \langle \Psi_{in} | (r\hat{a}_1^\dagger + t\hat{a}_2^\dagger) (r\hat{a}_1 + t\hat{a}_2) | \Psi_{in} \rangle \rightarrow \\ \rightarrow \langle 1|_1 \langle 0|_2 (r\hat{a}_1^\dagger + t\hat{a}_2^\dagger) (r\hat{a}_1 + t\hat{a}_2) |1\rangle_1 |0\rangle_2 = (r\sqrt{1} \langle 0|_1 \langle 0|_2 + 0) (r\sqrt{1} |0\rangle_1 |0\rangle_2 + 0) = r^2$$

2. Coincidences for a biphoton input:  $|\Psi_{in}\rangle = |1\rangle_1 |1\rangle_2$

$$\langle \Psi_{out} | \hat{a}_3^\dagger \hat{a}_4^\dagger \hat{a}_3 \hat{a}_4 | \Psi_{out} \rangle \rightarrow \langle 1|_1 \langle 1|_2 (r\hat{a}_1^\dagger + t\hat{a}_2^\dagger) (t\hat{a}_1^\dagger - r\hat{a}_2^\dagger) (r\hat{a}_1 + t\hat{a}_2) (t\hat{a}_1 - r\hat{a}_2) |1\rangle_1 |1\rangle_2 \rightarrow \\ \rightarrow \langle 0|_1 \langle 0|_2 (0 - \sqrt{1}\sqrt{1}r^2 + \sqrt{1}\sqrt{1}t^2 - 0) (0 - r^2\sqrt{1}\sqrt{1} + t^2\sqrt{1}\sqrt{1} - 0) |0\rangle_1 |0\rangle_2 = \\ = (t^2 - r^2)^2 = 0 \quad \text{if } r = t = 1/\sqrt{2}$$

If two undistinguishable photons are incident on a symmetric beam-splitter, they always exit the beam-splitter from the same port.

## B. Converting states (input to output)

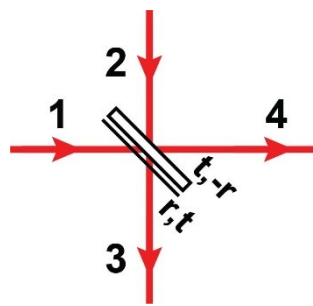
We will use number states as a basis for the Hilbert space of the system under consideration.

An example: input state is  $m$  photons at port 1 and  $q$  photons at port 2:

$$|\Psi_{in}\rangle = |m\rangle_1 |q\rangle_2$$

$$|\Psi_{in}\rangle = \frac{1}{\sqrt{m!}} \hat{a}_1^\dagger |m-1\rangle \frac{1}{\sqrt{q!}} \hat{a}_2^\dagger |q-1\rangle = \dots = \frac{1}{\sqrt{m!q!}} \left(\hat{a}_1^\dagger\right)^m \left(\hat{a}_2^\dagger\right)^q |0\rangle_1 |0\rangle_2$$

For a beam-splitter:



$$|\Psi_{in}\rangle = \frac{1}{\sqrt{m!q!}} \left(r\hat{a}_3^\dagger + t\hat{a}_4^\dagger\right)^m \left(t\hat{a}_3^\dagger - r\hat{a}_4^\dagger\right)^q |0\rangle_3 |0\rangle_4 = |\Psi_{out}\rangle$$

$$\text{For } m=1, q=0: \quad |\Psi_{out}\rangle = r|1\rangle_3 + t|1\rangle_4$$

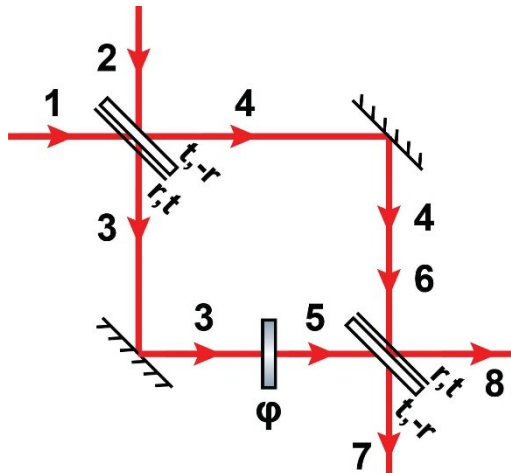
$$\text{For } m=1, q=1:$$

$$|\Psi_{out}\rangle = rt\sqrt{1}\sqrt{2}|2\rangle_3 |0\rangle_4 - rt\sqrt{1}\sqrt{2}|0\rangle_3 |2\rangle_4 + (t^2 - r^2)\sqrt{1}\sqrt{1}|1\rangle_3 |1\rangle_4$$

$$\begin{pmatrix} \hat{a}_1^\dagger \\ \hat{a}_2^\dagger \end{pmatrix} = \begin{pmatrix} r & t \\ t & -r \end{pmatrix} \begin{pmatrix} \hat{a}_3^\dagger \\ \hat{a}_4^\dagger \end{pmatrix}$$

$$\hat{a}_l |n\rangle_l = \sqrt{n} |n-1\rangle$$
$$\hat{a}_l^\dagger |n-1\rangle_l = \sqrt{n} |n\rangle$$

## B. Converting states (input to output)



Example: Mach-Zehnder Interferometer

$$\begin{pmatrix} \hat{a}_3^\dagger \\ \hat{a}_4^\dagger \end{pmatrix} = \begin{pmatrix} r & t \\ t & -r \end{pmatrix} \begin{pmatrix} \hat{a}_1^\dagger \\ \hat{a}_2^\dagger \end{pmatrix}$$

beam-splitter

$$\begin{pmatrix} \hat{a}_5^\dagger \\ \hat{a}_6^\dagger \end{pmatrix} = \begin{pmatrix} e^{+i\phi} & 0 \\ 0 & 1 \end{pmatrix} \begin{pmatrix} \hat{a}_3^\dagger \\ \hat{a}_4^\dagger \end{pmatrix}$$

delay (phase) added to  
one of the channels

$$\begin{pmatrix} \hat{a}_8^\dagger \\ \hat{a}_7^\dagger \end{pmatrix} = \begin{pmatrix} r & t \\ t & -r \end{pmatrix} \begin{pmatrix} \hat{a}_6^\dagger \\ \hat{a}_5^\dagger \end{pmatrix}$$

beam-splitter

**NB!** orientation changed!

$$\begin{pmatrix} \hat{a}_1^\dagger \\ \hat{a}_2^\dagger \end{pmatrix} = \begin{pmatrix} r & t \\ t & -r \end{pmatrix} \begin{pmatrix} \hat{a}_3^\dagger \\ \hat{a}_4^\dagger \end{pmatrix}$$

$$\begin{pmatrix} \hat{a}_3^\dagger \\ \hat{a}_4^\dagger \end{pmatrix} = \begin{pmatrix} e^{-i\phi} & 0 \\ 0 & 1 \end{pmatrix} \begin{pmatrix} \hat{a}_5^\dagger \\ \hat{a}_6^\dagger \end{pmatrix}$$

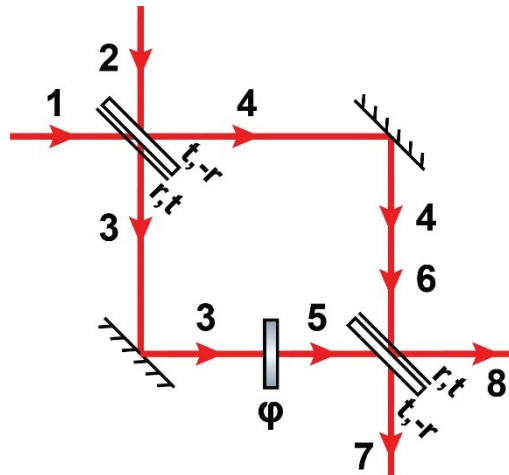
$$\begin{pmatrix} \hat{a}_5^\dagger \\ \hat{a}_6^\dagger \end{pmatrix} = \boxed{\begin{pmatrix} -r & t \\ t & r \end{pmatrix}} \begin{pmatrix} \hat{a}_7^\dagger \\ \hat{a}_8^\dagger \end{pmatrix}$$

$$|\Psi_{in}\rangle = |m\rangle_1 |q\rangle_2$$

$$\hat{a}_l |n\rangle_l = \sqrt{n} |n-1\rangle$$

$$\hat{a}_l^\dagger |n-1\rangle_l = \sqrt{n} |n\rangle$$

## B. Converting states (input to output)



Example: Mach-Zehnder Interferometer

$$\begin{pmatrix} \hat{a}_1^\dagger \\ \hat{a}_2^\dagger \end{pmatrix} = \begin{pmatrix} r & t \\ t & -r \end{pmatrix} \begin{pmatrix} \hat{a}_3^\dagger \\ \hat{a}_4^\dagger \end{pmatrix}$$

$$\begin{pmatrix} \hat{a}_3^\dagger \\ \hat{a}_4^\dagger \end{pmatrix} = \begin{pmatrix} e^{-i\phi} & 0 \\ 0 & 1 \end{pmatrix} \begin{pmatrix} \hat{a}_5^\dagger \\ \hat{a}_6^\dagger \end{pmatrix}$$

$$\begin{pmatrix} \hat{a}_5^\dagger \\ \hat{a}_6^\dagger \end{pmatrix} = \begin{pmatrix} -r & t \\ t & r \end{pmatrix} \begin{pmatrix} \hat{a}_7^\dagger \\ \hat{a}_8^\dagger \end{pmatrix}$$

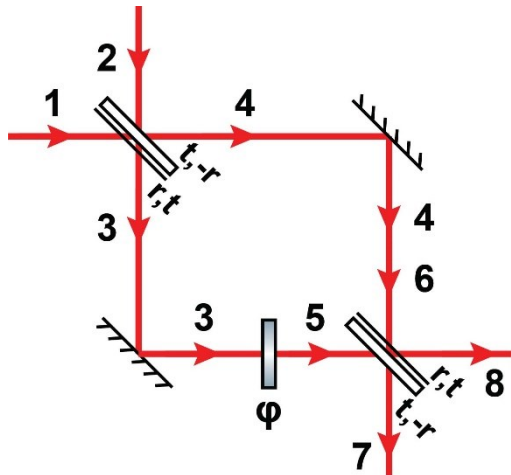
$$\begin{aligned}
 |\Psi_{in}\rangle &= \frac{1}{\sqrt{m!q!}} \left( r\hat{a}_3^\dagger + t\hat{a}_4^\dagger \right)^m \left( t\hat{a}_3^\dagger - r\hat{a}_4^\dagger \right)^q |0\rangle_3 |0\rangle_4 = \\
 &= \frac{1}{\sqrt{m!q!}} \left( re^{-i\phi} \left( -r\hat{a}_7^\dagger + t\hat{a}_8^\dagger \right) + t \left( t\hat{a}_7^\dagger + r\hat{a}_8^\dagger \right) \right)^m \cdot \\
 &\cdot \left( te^{-i\phi} \left( -r\hat{a}_7^\dagger + t\hat{a}_8^\dagger \right) - r \left( t\hat{a}_7^\dagger + r\hat{a}_8^\dagger \right) \right)^q |0\rangle_3 |0\rangle_4 = |\Psi_{out}\rangle
 \end{aligned}$$

$$|\Psi_{in}\rangle = |m\rangle_1 |q\rangle_2$$

$$\hat{a}_l |n\rangle_l = \sqrt{n} |n-1\rangle$$

$$\hat{a}_l^\dagger |n-1\rangle_l = \sqrt{n} |n\rangle$$

## B. Converting states (input to output)



Example: Mach-Zehnder Interferometer

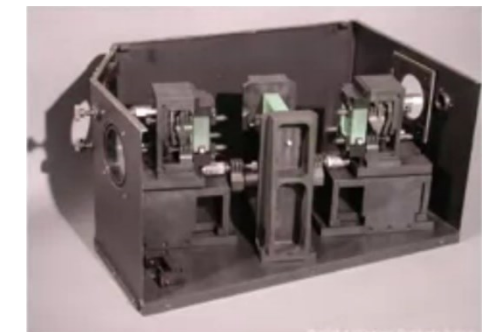
E.g., a single photon input:  $|\Psi_{in}\rangle = |1\rangle_1 |0\rangle_2$ ,  $m = 1, q = 0$

$$|\Psi_{out}\rangle = \frac{1}{\sqrt{m!q!}} \left( r e^{-i\phi} (-r\hat{a}_7^\dagger + t\hat{a}_8^\dagger) + t (t\hat{a}_7^\dagger + r\hat{a}_8^\dagger) \right) |0\rangle_3 |0\rangle_4 = \\ = (t^2 - r^2 e^{-i\phi}) |1\rangle_7 |0\rangle_8 + (rt + rte^{-i\phi}) |0\rangle_7 |1\rangle_8$$

Balanced interferometer:  $r = t = 1/\sqrt{2}$

$$|\Psi_{out}\rangle = e^{-i\phi/2} \frac{e^{+i\phi/2} - e^{-i\phi/2}}{2} |1\rangle_7 |0\rangle_8 + e^{-i\phi/2} \frac{e^{+i\phi/2} + e^{-i\phi/2}}{2} |0\rangle_7 |1\rangle_8$$

$$|\Phi_{out}\rangle = i \sin(\phi/2) |1\rangle_7 |0\rangle_8 + \cos(\phi/2) |0\rangle_7 |1\rangle_8$$



Probability to detect a photon in channel 7:

$$P(|1\rangle_7) = |\langle 1|_7 |\Phi\rangle_{out}|^2 = \sin^2(\phi/2)$$

**Interferometer works as such even at the single-photon level.**

$$|\Psi_{in}\rangle = \frac{1}{\sqrt{m!q!}} \left( r e^{-i\phi} (-r\hat{a}_7^\dagger + t\hat{a}_8^\dagger) + t (t\hat{a}_7^\dagger + r\hat{a}_8^\dagger) \right)^m \cdot \\ \cdot \left( t e^{-i\phi} (-r\hat{a}_7^\dagger + t\hat{a}_8^\dagger) - r (t\hat{a}_7^\dagger + r\hat{a}_8^\dagger) \right)^q |0\rangle_3 |0\rangle_4 = |\Psi_{out}\rangle$$

## C. Probabilistic optical CNOT gate

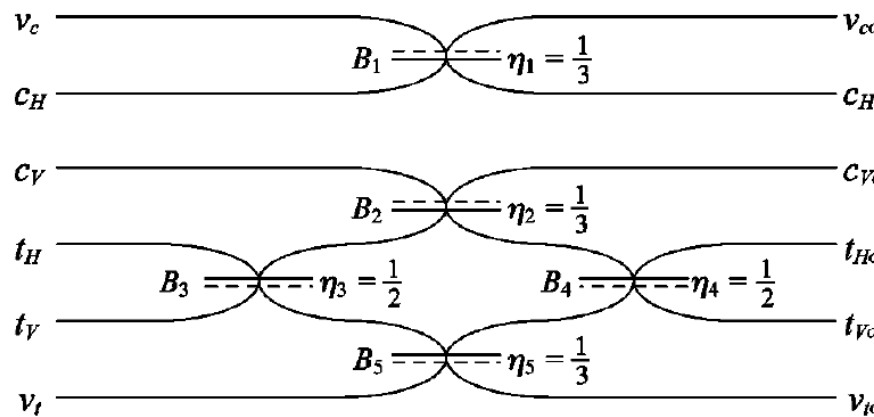
in:

In: qubit 1 (cH, cV), qubit 2 (tH, tV)

“v”: vacuum, no input, not detected

Beam-splitters:  $r^2 = \eta$ .

$$\begin{aligned} |\phi\rangle &= (\alpha|HH\rangle + \beta|HV\rangle + \gamma|VH\rangle + \delta|VV\rangle)|00\rangle \\ &= (\alpha c_H^\dagger t_H^\dagger + \beta c_H^\dagger t_V^\dagger + \gamma c_V^\dagger t_H^\dagger \\ &\quad + \delta c_V^\dagger t_V^\dagger)|0000\rangle|00\rangle \end{aligned}$$



out:

$$|\phi\rangle_{out} = (\alpha c_{Ho}^\dagger t_{Ho}^\dagger + \beta c_{Ho}^\dagger t_{Vo}^\dagger + \gamma c_{Vo}^\dagger t_{Ho}^\dagger + \delta c_{Vo}^\dagger t_{Vo}^\dagger)|0000\rangle|00\rangle$$

$$\begin{aligned} &= \frac{1}{3}\{\alpha|HH\rangle + \beta|HV\rangle + \gamma|VH\rangle + \delta|VV\rangle + \sqrt{2}(\alpha+\beta)|0100\rangle|10\rangle + \sqrt{2}(\alpha-\beta)|0000\rangle|11\rangle + (\alpha+\beta)|1100\rangle|00\rangle \\ &\quad + (\alpha-\beta)|1000\rangle|01\rangle + \sqrt{2}\alpha|0010\rangle|10\rangle + \sqrt{2}\beta|0001\rangle|10\rangle - \sqrt{2}(\gamma+\delta)|0200\rangle|00\rangle - (\gamma-\delta)|0100\rangle|01\rangle \\ &\quad + \sqrt{2}\gamma|0020\rangle|00\rangle + (\gamma-\delta)|0010\rangle|01\rangle + (\gamma+\delta)|0011\rangle|00\rangle + (\gamma-\delta)|0001\rangle|01\rangle + \sqrt{2}\delta|0002\rangle|00\rangle\} \end{aligned}$$

$$c_{Ho} = \frac{1}{\sqrt{3}}(\sqrt{2}v_c + c_H),$$

$$c_{Vo} = \frac{1}{\sqrt{3}}(-c_V + t_H + t_V),$$

$$t_{Ho} = \frac{1}{\sqrt{3}}(c_V + t_H + v_t),$$

$$t_{Vo} = \frac{1}{\sqrt{3}}(c_V + t_V - v_t),$$

$$v_{co} = \frac{1}{\sqrt{3}}(-v_c + \sqrt{2}c_H),$$

$$v_{to} = \frac{1}{\sqrt{3}}(t_H - t_V - v_t).$$



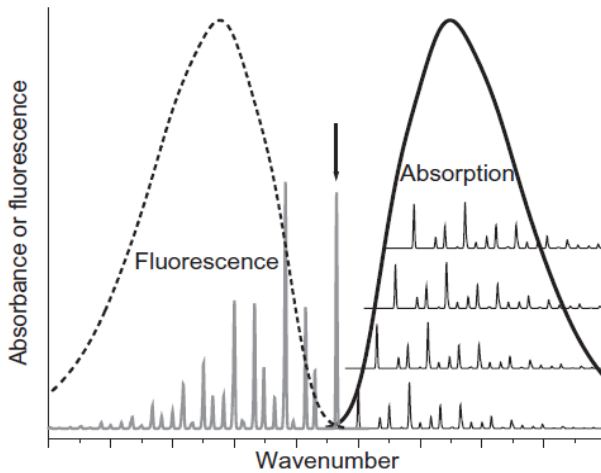
## Media-based QM:

- Optically controlled:
  - Electromagnetically induced transparency (EIT)
  - Raman
- Engineered absorption:
  - Controlled reversible inhomogeneous broadening (CRIB)
  - Atomic frequency combs (AFC)
- Hybrid type

## Notions to be introduced:

- Energy diagrams;
- Homogeneous and inhomogeneous line broadening;
- Optical photon echo in systems with inhomogeneous line broadening.

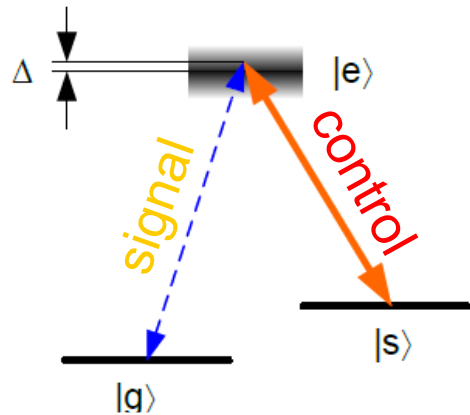
# Line broadening mechanisms:



- Homogeneous broadening:  
affects every particle in the ensemble in the same way. Energy level structure is the same for all the particles.  
Mechanisms, e.g.: natural broadening (energy level lifetime).
  
- Inhomogeneous broadening:  
every particle has its own, slightly different energy level structure. Total spectrum is the superposition of individual (but sharp!) spectra.  
Mechanisms, e.g.: Doppler broadening (molecules in a gas).

# Media-based QM — 1: optically-controlled

## Electromagnetically induced transparency (EIT)



$\Lambda$  (lambda)-type three-energy-level structure  
 $|g\rangle$  to  $|s\rangle$ : ED forbidden

Bandwidth:

0.1 MHz (warm atoms)  
10 MHz (cold atoms)

GHz (Cs, Rb)  
THz (NV-centres, H<sub>2</sub>)

1. Strong control pulse ( $\rightarrow |g\rangle$ )
2. Control + signal pulse ( $\rightarrow |s\rangle$ ) ("stationary qubit")
3. After storage: retrieval control pulse ( $\rightarrow |g\rangle$ ) => "flying qubit"

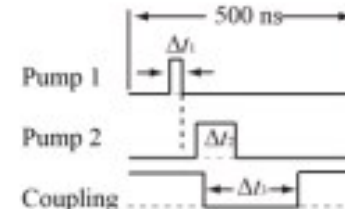
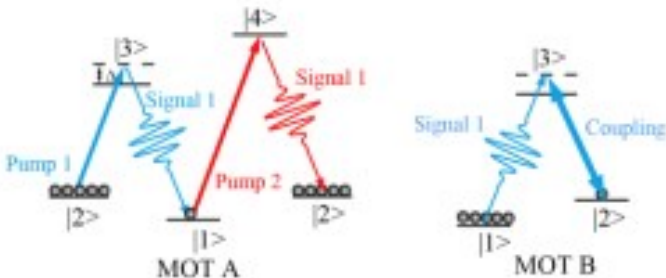
Demonstrated in:

- ❖ single atoms
- ❖ warm atomic vapors
- ❖ laser-trapped cold atoms
- ❖ Bose-Einstein condensates (BECs)
- ❖ rare-earth-doped solid state materials

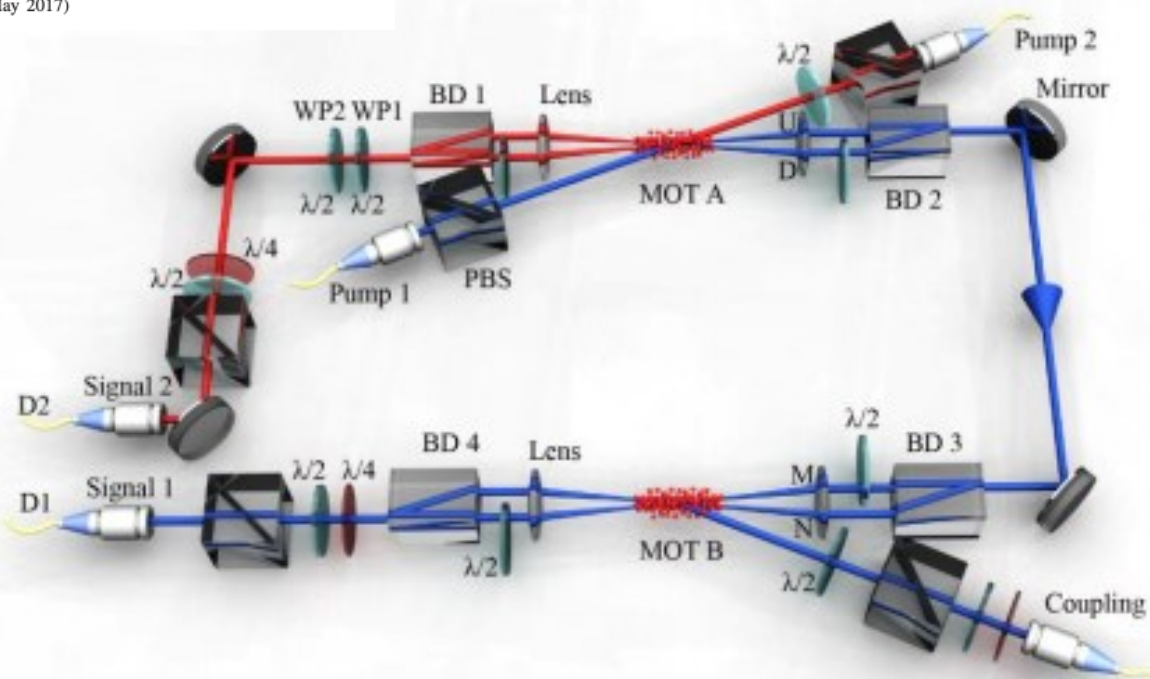
## Quantum Secure Direct Communication with Quantum Memory

Wei Zhang,<sup>1,3</sup> Dong-Sheng Ding,<sup>1,3,\*</sup> Yu-Bo Sheng,<sup>2,†</sup> Lan Zhou,<sup>2</sup> Bao-Sen Shi,<sup>1,3,‡</sup> and Guang-Can Guo<sup>1,3</sup><sup>1</sup>*Key Laboratory of Quantum Information, Chinese Academy of Sciences,**University of Science and Technology of China, Hefei, Anhui 230026, China*<sup>2</sup>*Key Laboratory of Broadband Wireless Communication and Sensor Network Technology,  
Nanjing University of Posts and Telecommunications, Ministry of Education, Nanjing 210003, China*<sup>3</sup>*Synergetic Innovation Center of Quantum Information and Quantum Physics,**University of Science and Technology of China, Hefei, Anhui 230026, China*

(Received 14 October 2016; published 31 May 2017)



(a)



# Media-based QM — 2: engineered absorption-1

## Photon echo

- A system with only 2 active energy levels is excited at  $t = 0$ .
- Distance between the levels vary inhomogeneously:  $\Delta E = \hbar (\omega + \delta)$
- Evolution of each of the particles depends on the  $\Delta E$  value  
=> decoherence.
- Evolution of the system can be reversed using a pulse of electromagnetic field of a certain duration, sent at time  $t = t_1$ .
- Coherence is restored and system is re-emitting the stored energy after  $t = 2t_1$ .

[ A.M. Kelley. (2012). *Condensed-Phase Molecular Spectroscopy and Photophysics*. New Jersey: John Wiley & Sons, Inc. ] (Sec. 11.7 “Photon Echoes”)

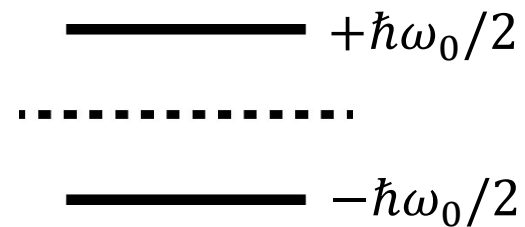
[ D. Klyshko. (2011). *Physical Foundations of Quantum Electronics*. (Eds. M. Chekhova, S. Kulik). <https://doi.org/10.1142/7930> ]

[A. Yariv. (1975). *Quantum Electronics* (2nd ed.). New York: John Wiley & Sons. ]

# Photon echo

2D Hilbert space

**Heisenberg picture:**  $\rho = \text{const}(t)$



**Pauli matrices:**  $\sigma_x \equiv \begin{pmatrix} 0 & 1 \\ 1 & 0 \end{pmatrix}$ ,  $\sigma_y \equiv \begin{pmatrix} 0 & -i \\ i & 0 \end{pmatrix}$ ,  $\sigma_z \equiv \begin{pmatrix} 1 & 0 \\ 0 & -1 \end{pmatrix}$ .

If  $\sigma_j$  is in the energy basis:  $\hat{\mathcal{H}}_0 = -h\bar{\omega}_0 \hat{\sigma}_z / 2$

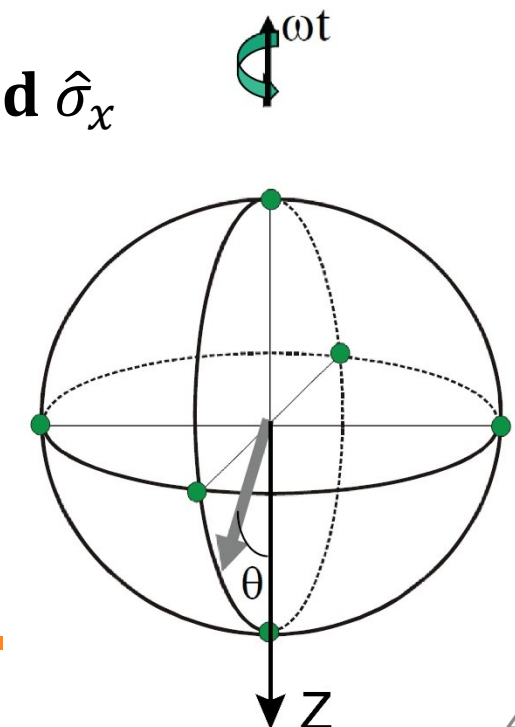
Dipole moment of a non-polar molecule:  $\hat{\mathbf{d}} = \mathbf{d} \hat{\sigma}_x$

Relative inversion:  $\langle \hat{\sigma}_z \rangle = \rho_{11} - \rho_{22} = \Delta$

Perturbation operator:  $\hat{V} = -(\mathbf{d}_0, \mathbf{E}) \hat{\sigma}_x$

Bloch vector and Bloch sphere:

$$\mathbf{R} = \langle \hat{\boldsymbol{\sigma}} \rangle = \{2\text{Re}(\rho_{21}), 2\text{Im}(\rho_{21}), \Delta\}$$



# Photon echo

Bloch vector and Bloch sphere:

$$\mathbf{R} = \langle \hat{\sigma} \rangle = \{2\text{Re}(\rho_{21}), 2\text{Im}(\rho_{21}), \Delta\}$$

$$\mathbf{R}^2 = 4|\rho_{12}|^2 + (\rho_{11} - \rho_{22})^2$$

Pure state:  $|\rho_{12}|^2 = \rho_{12}^* \rho_{12} \rightarrow b_1^* b_2 \ b_2^* b_1 = \rho_{11} \rho_{22}$  and  $\mathbf{R}^2 = 1$ .

Mixed state:  $\mathbf{R}^2 < 1$ .

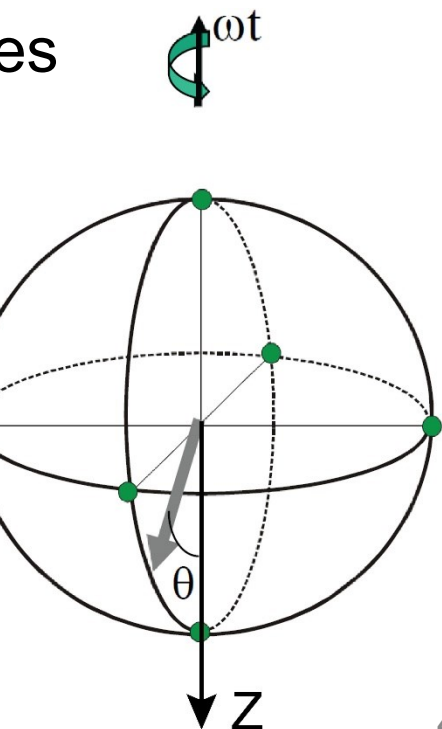
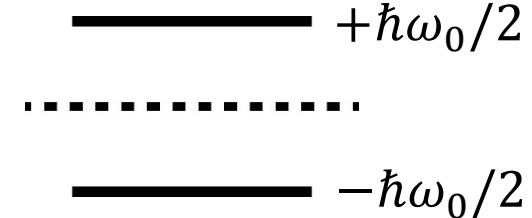
equator  $\rightarrow$  coherent states  
sphere  $\rightarrow$  pure states

Evolution:

$$i\hbar \frac{\partial \hat{V}}{\partial t} = [\hat{V}, \hat{\mathcal{H}}] \quad \hat{V} = -(\mathbf{d}_0, \mathbf{E}) \hat{\sigma}_x$$

$$\dot{\mathbf{R}} = [\mathbf{R} \times \mathbf{A}] \quad \mathbf{A} = \{\Omega_R(t), 0, \omega_0\}$$

$$\Omega_R = \frac{2d_0}{\hbar} E(t) \quad \text{Rabi frequency}$$



# Photon echo

$$\dot{\mathbf{R}} = [\mathbf{R} \times \mathbf{A}] - \mathbf{R}_\perp/T_2 - \hat{\mathbf{z}}(R_z - \Delta_0)/T_1$$

$$\mathbf{A} = \{\Omega_R(t), 0, \omega_0\} \quad \Omega_R = \frac{2d_0}{\hbar} E(t)$$

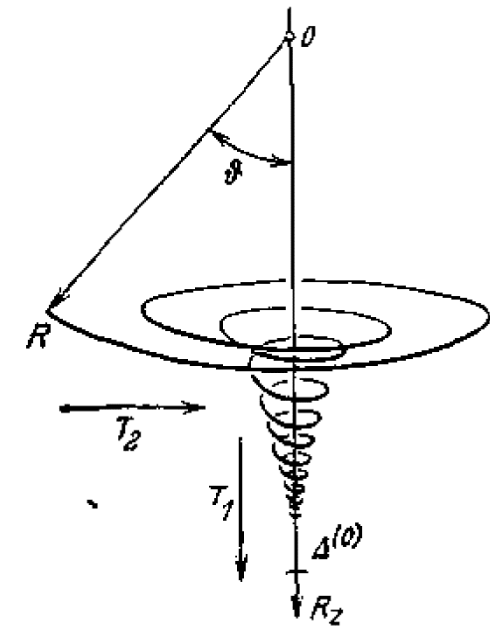
$$E(t) = (1/2)E_0(t)e^{-i\omega t + \varphi} + c.c.$$

$$\Delta = R_z = \Delta_0 \left( 1 - 2 \left[ \frac{\Omega}{\tilde{\Omega}} \sin \left( \frac{\tilde{\Omega}t}{2} \right) \right]^2 \right)$$

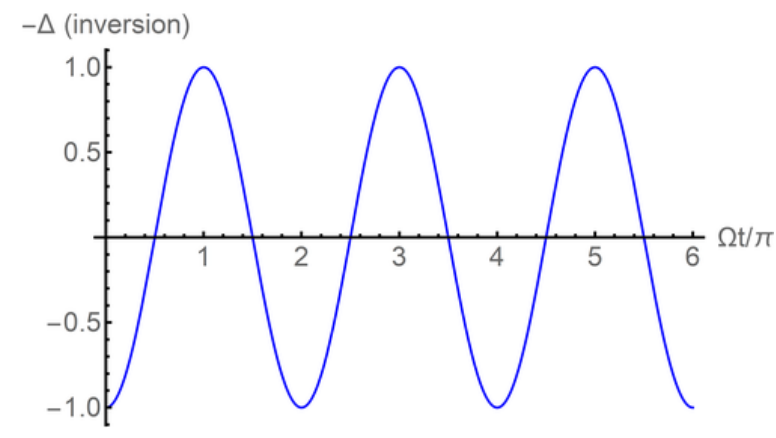
$$\tilde{\Omega}^2 = \Omega^2 + (\omega - \omega_0)^2$$

$-\Delta/\Delta_0 = -\cos(\Omega t)$ : relative inversion

$\pi$ -pulse:  $\Omega t_\pi = \pi \quad t_\pi = \frac{\pi}{\Omega} = \frac{\hbar}{2d_0 E}$



Evolution of  $\Delta/\Delta_0$ :



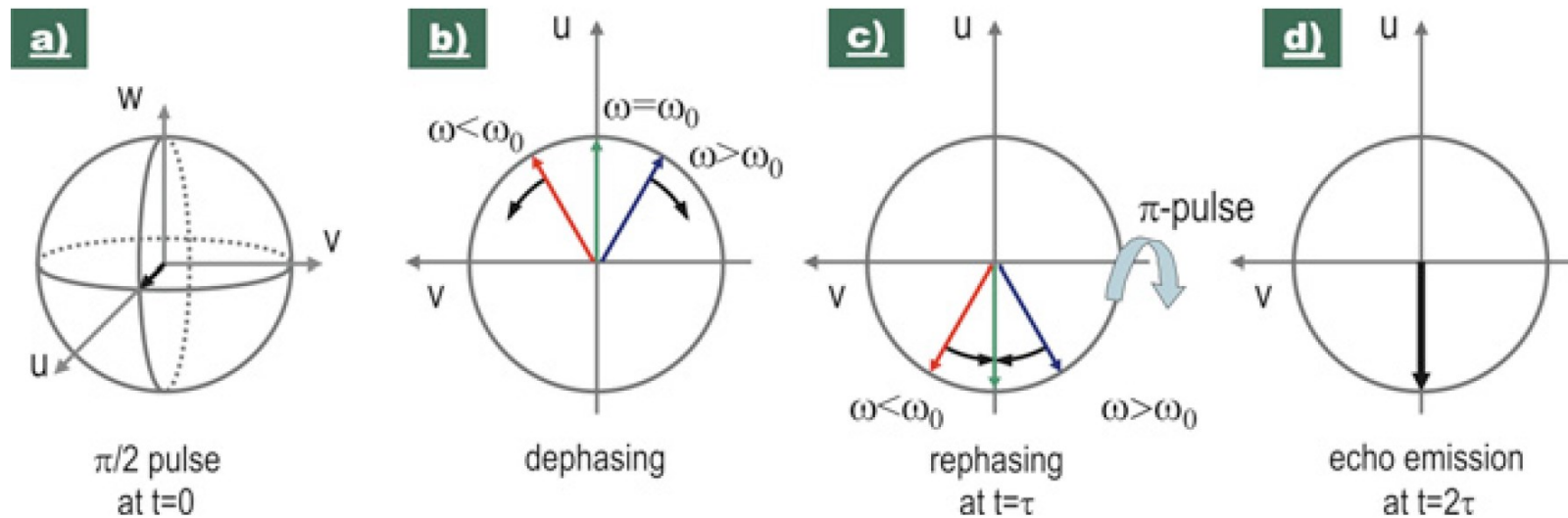
# Photon echo

$$\dot{\mathbf{R}} = [\mathbf{R} \times \mathbf{A}] - \mathbf{R}_\perp/T_2 - \hat{\mathbf{z}}(R_z - \Delta_0)/T_1$$

$$\mathbf{A} = \{\Omega_R(t), 0, \omega_0\} \quad \Omega_R = \frac{2d_0}{\hbar} E(t)$$

$$E(t) = (1/2)E_0(t)e^{-i\omega t + \varphi} + c.c.$$

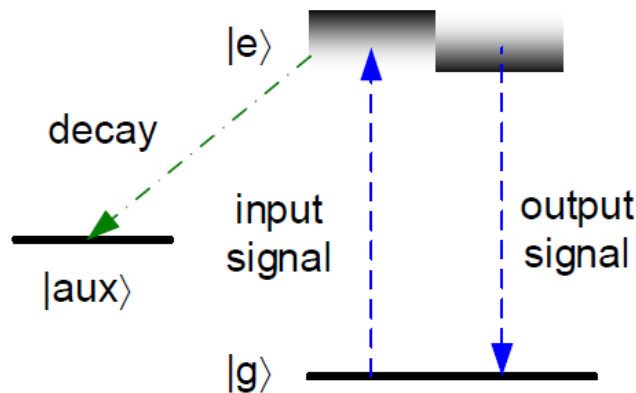
Inhomogeneous broadening:  
 $\omega_0 \neq \text{const}$  in the ensemble.



[ W. Tittel, M. Afzelius, T. Chaneliere, R.L. Cone, S. Kroell, S.A. Moiseev, M. Sellars, "Photon-echo quantum memory in solid state systems" // *Laser & Photonics Reviews* **4** (2), 244–267 (2010); DOI 10.1002/lpor.200810056 .. ]

# Media-based QM — 2: engineered absorption-1

## Controlled reversible inhomogeneous broadening (CRIB)

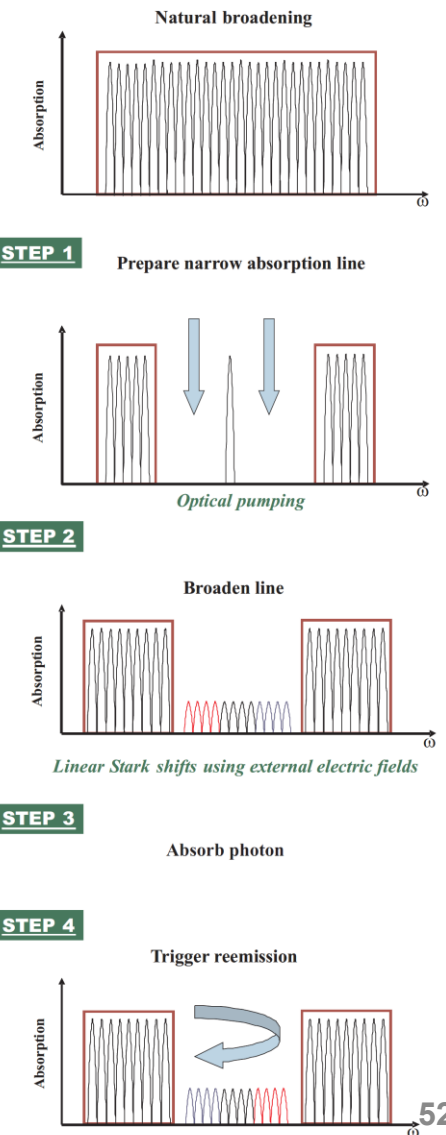


- Pump wave + spectral hole burning inhomogeneous broadening (E, H).
- External state is stored.
- Retrieval: broadening field reversal => => photon echo.



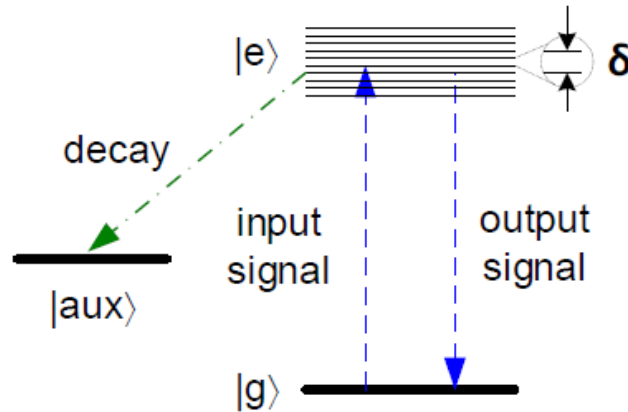
Aalto University

[ W. Tittel, M. Afzelius, T. Chaneliere, R.L. Cone, S. Kroell, S.A. Moiseev, M. Sellars, "Photon-echo quantum memory in solid state systems" // *Laser & Photonics Reviews* 4 (2), 244–267 (2010); DOI 10.1002/lpor.200810056 .. ]

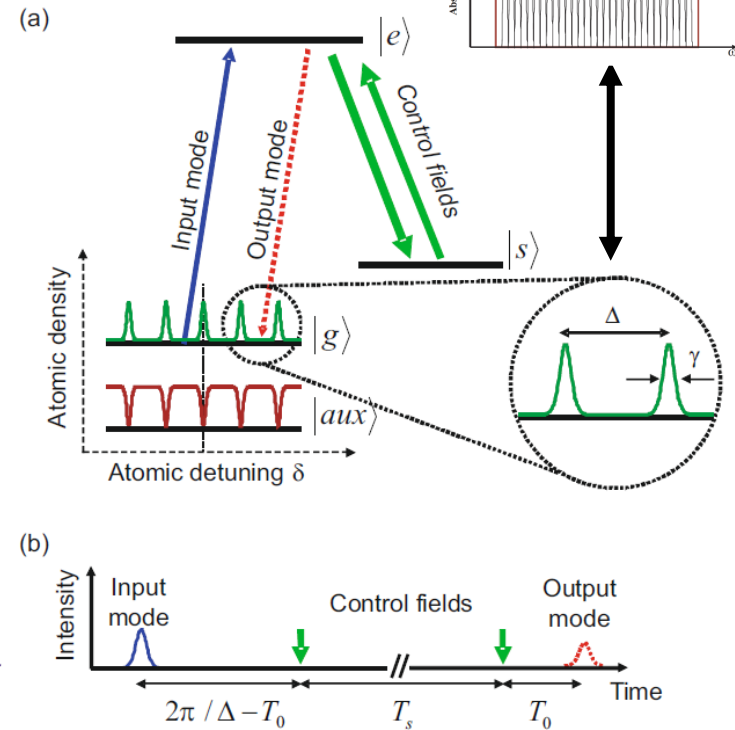
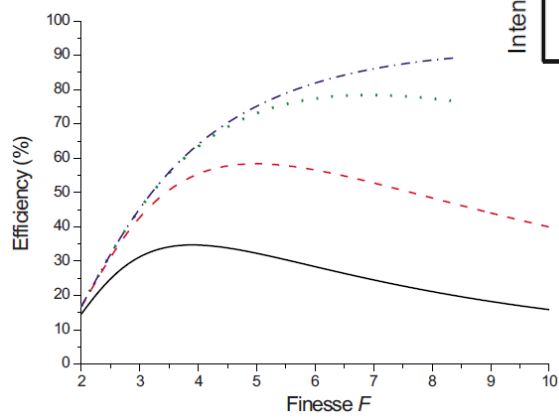
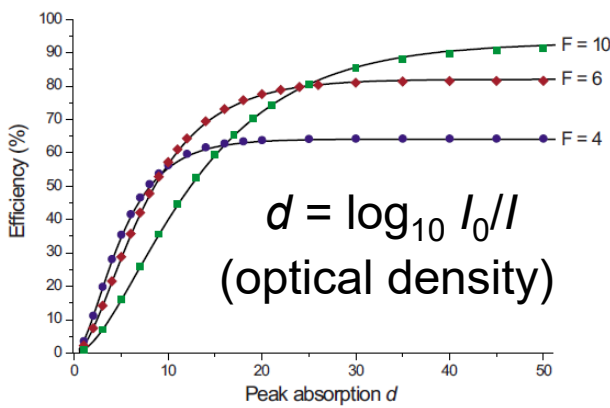


# Media-based QM — 2: engineered absorption-2

## Atomic frequency combs (AFC)



structuring the atomic density of states (DoS)

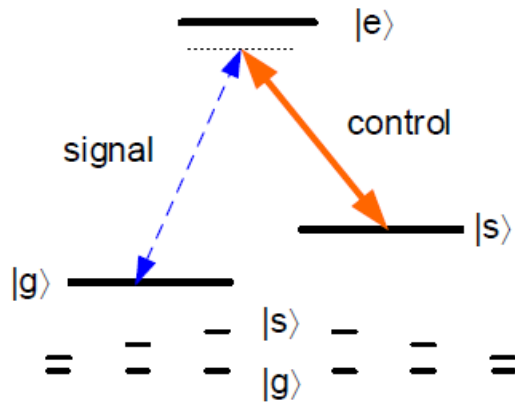


Finesse:  $F = \Delta / \gamma$ .

Efficiency:

$$\eta_{AFC} \approx \left(1 - e^{-d}\right)^2 e^{-\frac{7}{F^2}}$$

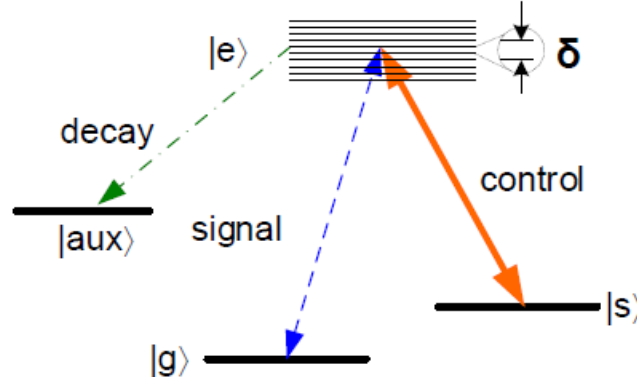
## Media-based QM — 3: hybrid approach



**Raman-GEM (CRIB)**  
(gradient echo memory)

inherently narrow lines  
(spin levels)

**Future prospects:**  
macroscopic optomechanical oscillators ?



**Λ-AFC**

introduced on-demand  
capability

longer storage time  
multimode

**Optical and spin manipulation of non-Kramers rare-earth ions in a weak magnetic field  
for quantum memory applications**

J. Etesse <sup>1,\*</sup> A. Holzapfel <sup>2</sup>, A. Ortu <sup>2</sup> and M. Afzelius <sup>2</sup>

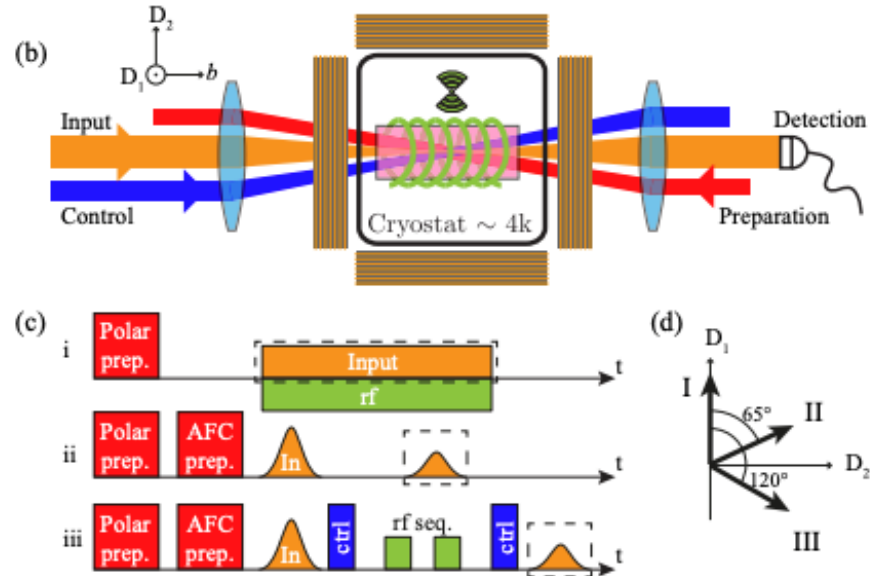
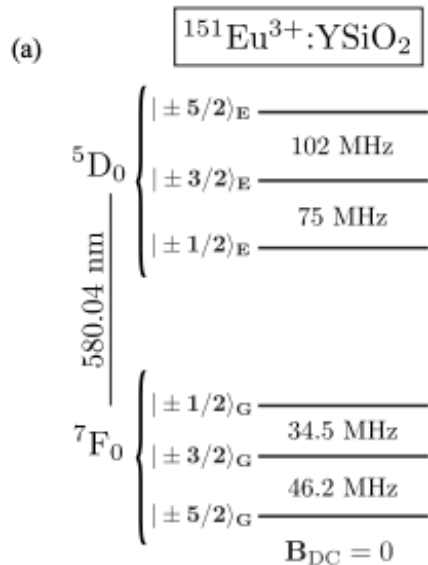
<sup>1</sup>Université côte d'Azur, CNRS, Institut de Physique de Nice (INPHYNI), UMR 7010, Parc Valrose, Nice Cedex 2, France

<sup>2</sup>Department of Applied Physics, University of Geneva, CH-1211 Geneva 4, Switzerland

(Received 12 November 2020; accepted 29 January 2021; published 26 February 2021)

Rare-earth ion doped crystals have proven to be solid platforms for implementing quantum memories. Their potential use for integrated photonics with large multiplexing capability and unprecedented coherence times is at the core of their attractiveness. The best performances of these ions are, however, usually obtained when subjected to a DC magnetic field, but consequences of such fields on the quantum memory protocols have only received little attention. In this paper, we focus on the effect of a DC bias magnetic field on the population manipulation of non-Kramers ions with nuclear quadrupole states, both in the spin and optical domains, by developing a simple theoretical model. We apply this model to explain experimental observations in a  $^{151}\text{Eu}^3+\text{:YSiO}_2$  crystal, and highlight specific consequences on the atomic frequency comb spin-wave protocol. The developed analysis should allow predicting optimal magnetic field configurations for various protocols.

DOI: 10.1103/PhysRevA.103.022618



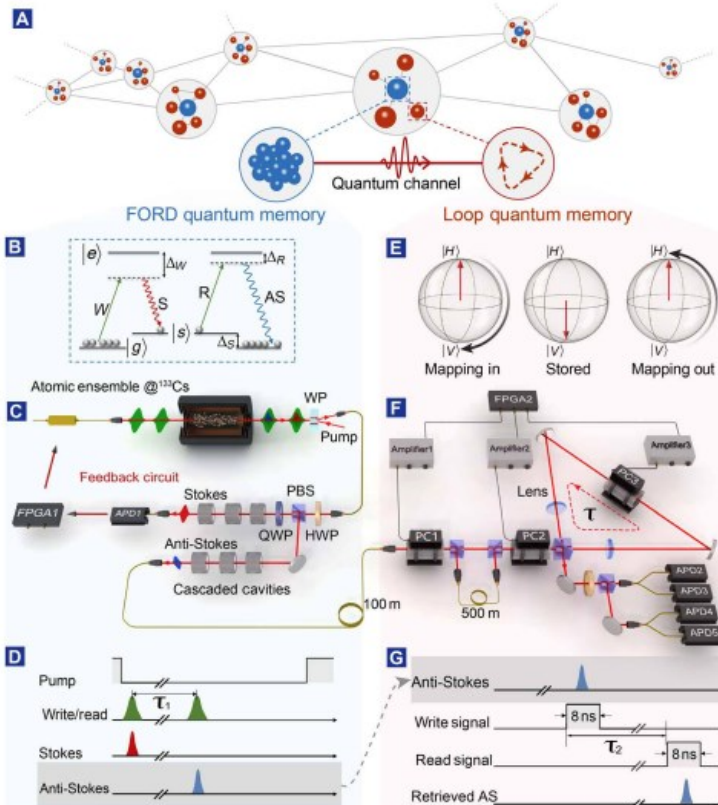
Doped solid-state crystal in a helium cryostat (4K) with optical inputs

## A hybrid quantum memory–enabled network at room temperature

Xiao-Ling Pang<sup>1,2</sup>, Ai-Lin Yang<sup>1,2</sup>, Jian-Peng Dou<sup>1,2</sup>, Hang Li<sup>1,2</sup>, Chao-Ni Zhang<sup>1,2</sup>, Eilon Poem<sup>3,4</sup>, Dylan J. Saunders<sup>3</sup>, Hao Tang<sup>1,2</sup>, Joshua Nunn<sup>3,5</sup>, Ian A. Walmsley<sup>3</sup>, Xian-Min Jin<sup>1,2,6\*</sup>

Quantum memory capable of storage and retrieval of flying photons on demand is crucial for developing quantum information technologies. However, the devices needed for long-distance links are different from those envisioned for local processing. We present the first hybrid quantum memory-enabled network by demonstrating the interconnection and simultaneous operation of two types of quantum memory: an atomic ensemble-based memory and an all-optical Loop memory. Interfacing the quantum memories at room temperature, we observe a well-preserved quantum correlation and a violation of Cauchy-Schwarz inequality. Furthermore, we demonstrate the creation and storage of a fully-operable heralded photon chain state that can achieve memory-built-in combining, swapping, splitting, tuning, and chopping single photons in a chain temporally. Such a quantum network allows atomic excitations to be generated, stored, and converted to broadband photons, which are then transferred to the next node, stored, and faithfully retrieved, all at high speed and in a programmable fashion.

Copyright © 2020  
The Authors, some  
rights reserved;  
exclusive licensee  
American Association  
for the Advancement  
of Science. No claim to  
original U.S. Government  
Works. Distributed  
under a Creative  
Commons Attribution  
NonCommercial  
License 4.0 (CC BY-NC).



Recently, we have realized a broadband and room temperature far off-resonance **DLCZ (FORD) quantum memory**, capable of operating with a high fidelity in the quantum regime. Now, we are pursuing a quantum memory that is broadband, room temperature, and more importantly, compatible with the FORD quantum memory for further storing Stokes/anti-Stokes photons (i.e., mapping in) and retrieving them (i.e., mapping out) for controlled durations without any additional noise. **Progress toward such a memory has been made by using excited states of atoms**, albeit with a limited lifetime.

**Fig. 1. A schematic diagram and experimental setup for a hybrid quantum memory enabled network.** (A) A quantum network consists of two different functional nodes and their interconnections. (B) Write and read processes of FORD quantum memory. Solid lines represent three-level  $\Lambda$ -type configuration of atoms, in which states  $|g\rangle$  and  $|s\rangle$  are hyperfine ground states of cesium atoms ( $\Delta_g = 9.2$  GHz); state  $|e\rangle$  is the excited state; dashed lines represent broad virtual energy levels induced by the write and read pulses. (C) Setup of FORD quantum memory. WP, Wollaston prism; PBS, polarization beam splitter; QWP, quarter wave plate; HWP, half wave plate. (D) Time sequences of FORD quantum memory. (E) Polarization switching in the mapping in-and-out processes shown in Bloch spheres. (F) Setup of Loop quantum memory. The Pockels cell in the loop is controlled by write and read electrical signals from two channels of a field-programmable gate array (FPGA) module. A 500-m-long fiber is introduced to coordinate with the Loop memory as another switching path against photon loss. Four avalanche photodiodes (APDs) are used to detect photons in a chain with small time interval. PC, Pockels cells. (G) Time sequences of Loop memory. The time interval  $\tau_2$  between write and read signals can be any positive integral multiples of 1 cycle period  $\tau$ .

## A Ten-Qubit Solid-State Spin Register with Quantum Memory up to One Minute

C. E. Bradley,<sup>1,2,†</sup> J. Randall,<sup>1,2,†</sup> M. H. Abobeih,<sup>1,2</sup> R. C. Berrevoets,<sup>1,2</sup> M. J. Degen,<sup>1,2</sup>  
M. A. Bakker,<sup>1,2</sup> M. M. Markham,<sup>3</sup> D. J. Twitchen,<sup>3</sup> and T. H. Taminiau<sup>1,2,\*</sup>

<sup>1</sup>QuTech, Delft University of Technology, P.O. Box 5046, 2600 GA Delft, Netherlands

<sup>2</sup>Kavli Institute of Nanoscience Delft, Delft University of Technology,

P.O. Box 5046, 2600 GA Delft, Netherlands

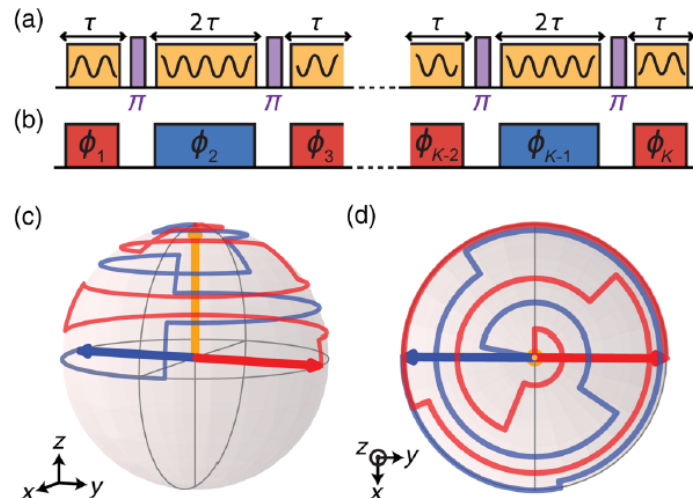
<sup>3</sup>Element Six, Fermi Avenue, Harwell Oxford, Didcot, Oxfordshire, OX11 0QR, United Kingdom

(Received 9 May 2019; published 11 September 2019)

Spins associated with single defects in solids provide promising qubits for quantum-information processing and quantum networks. Recent experiments have demonstrated long coherence times, high-fidelity operations, and long-range entanglement. However, control has so far been limited to a few qubits, with entangled states of three spins demonstrated. Realizing larger multiqubit registers is challenging due to the need for quantum gates that avoid cross talk and protect the coherence of the complete register. In this paper, we present novel decoherence-protected gates that combine dynamical decoupling of an electron spin with selective phase-controlled driving of nuclear spins. We use these gates to realize a ten-qubit quantum register consisting of the electron spin of a nitrogen-vacancy center and nine nuclear spins in diamond. We show that the register is fully connected by generating entanglement between all 45 possible qubit pairs and realize genuine multipartite entangled states with up to seven qubits. Finally, we investigate the register as a multiqubit memory. We demonstrate the protection of an arbitrary single-qubit state for over 75 s—the longest reported for a single solid-state qubit—and show that two-qubit entanglement can be preserved for over 10 s. Our results enable the control of large quantum registers with long coherence times and therefore open the door to advanced quantum algorithms and quantum networks with solid-state spin qubits.

DOI: 10.1103/PhysRevX.9.031045

Subject Areas: Condensed Matter Physics,  
Quantum Physics,  
Quantum Information



C. E. BRADLEY *et al.*

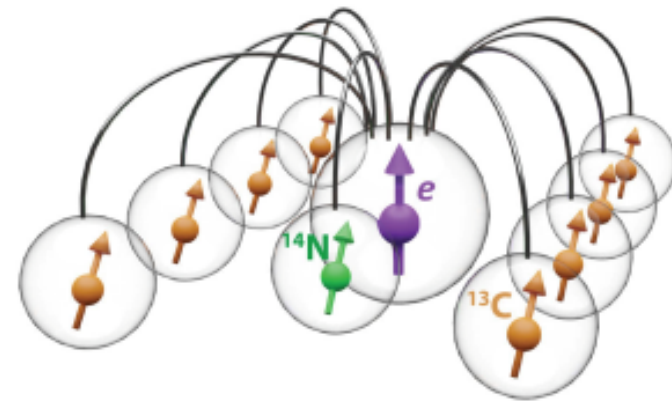


FIG. 1. Illustration of the ten-qubit register developed in this work. The electron spin of a single NV center in diamond acts as a central qubit and is connected by two-qubit gates to the intrinsic <sup>14</sup>N nuclear spin and a further eight <sup>13</sup>C nuclear spins surrounding the NV center.

# Highly efficient optical quantum memory with long coherence time in cold atoms

Y.-W. CHO,<sup>1</sup> G. T. CAMPBELL,<sup>1</sup> J. L. EVERETT,<sup>1</sup> J. BERNU,<sup>1</sup> D. B. HIGGINBOTTOM,<sup>1</sup> M. T. CAO,<sup>1</sup> J. GENG,<sup>1</sup> N. P. ROBINS,<sup>2</sup> P. K. LAM,<sup>1</sup> AND B. C. BUCHLER<sup>1,\*</sup>

<sup>1</sup>Centre for Quantum Computation and Communication Technology, Department of Quantum Science, The Australian National University, Canberra, ACT 0200, Australia

<sup>2</sup>Department of Quantum Science, The Australian National University, Canberra, ACT 0200, Australia

\*Corresponding author: ben.buchler@anu.edu.au

